Nuclear Physics B175 (1980) 365–401

HIGH-ENERGY BEHAVIOUR IN A NON-ABELIAN GAUGE THEORY (II). First corrections to $T_{n\to m}$ beyond the leading ln s approximation

J. BARTELS

II. Institut für Theoretische Physik der Universität Hamburg, Germany

Received 26 March 1980

In this second part of our attempt to construct a unitary high-energy description of a spontaneously broken non-abelian gauge theory we calculate, for the $n\to m$ amplitude in the multi-Regge limit, the first corrections beyond the leading logarithmic approximation. The resulting amplitudes come in the form of the reggeon calculus where the number of reggeons in each t-channel is restricted to one or two. We then study the limit where the mass of the vector particle is taken to zero: for the $2\to 2$ amplitude we show that this limit exists, not only for the approximation of the present paper but also for higher-order corrections.

1. Introduction

In a previous paper [1] (henceforth referred to as I) we have started a program whose aim is the construction of an acceptable high-energy description of spontaneously broken non-abelian gauge theories. The main motivation for this came from the observation [2, 3] that, quite similar to the situation in abelian theories (QED), the leading logarithmic approximation (LLA) for the vacuum quantum number exchange channel (pomeron) violates the Froissart bound and, hence, does not obey s-channel unitarity. An acceptable high-energy theory, therefore, must necessarily go beyond this approximation, and it is mandatory that unitarity is fully incorporated. This suggests the use of unitarity from the start: the lagrangian determines certain tree elements, and all loop corrections are constructed from discontinuities, i.e., dispersion relations and unitarity equations. In I this method was introduced and, as the first step, used for the construction of $n\to m$ amplitudes in the leading logarithmic approximation. In the present paper we continue these calculations and construct the first non-leading corrections to the LLA, as they are required by unitarity.

The main results of I can be summarized as follows. We have been working in the SU(2) Higgs model where, after spontaneous symmetry breaking, a global SU(2) symmetry (called isospin) is left and all vector particles have the same mass M. The $m\to n$ amplitudes in the LLA are found to have simple multi-Regge

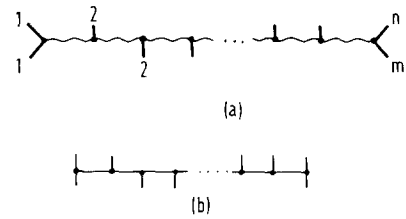

Fig. 1. The $n \to m$ amplitude in the leading-logarithmic approximation: (a) the wavy lines denote the exchange of the reggeized vector particle; (b) the group weight diagram.

behavior (fig. 1): all t-channels have odd signature and carry the quantum number of the reggeizing vector particle. This generalizes the property of reggeization which first was established on the level of the Born approximation for the $2 \to 2$ amplitude by Grisaru et al. [4]. A non-trivial feature of this result for the $n \to m$ amplitudes is the absence of multi-Regge cuts. Signature conservation would not exclude such cut contributions in one of the internal exchange channels of fig. 1, but, as a result of rather subtle cancellations, they do not contribute to the LLA. In the final part of I the unitarity properties of the LLA were demonstrated: all energy discontinuities (for the total energy as well as for all subenergy variables) are in agreement with unitarity, for example:

$$\mathrm{disc}_s T_{2\to 2} = \tfrac{1}{2} \sum_n \int \mathrm{d}\Omega_n |T_{2\to n}|^2_{\text{odd signature}}, \tag{1.1}$$

$$\mathrm{disc}_{s_{ab}} T_{2\to 3} = \tfrac{1}{2} \sum_n \int \mathrm{d}\Omega_n T_{2\to n+1} T^*_{2\to n \text{ odd signature}}, \tag{1.2}$$

$$\mathrm{disc}_s T_{2\to 3} = \tfrac{1}{2} \sum_n \int \mathrm{d}\Omega_n T_{2\to n} T^*_{3\to n \text{ odd signature}}. \tag{1.3}$$

On the r.h.s. of these equations, however, all t-channels are restricted to odd signature exchanges or, equivalently, to the quantum number of the vector particles, which does not allow for the pomeron yet. Eqs. (1.1)–(1.3) can be written in a more compact form. We denote by $T^{(1)}$ the matrix whose elements are the $n \to m$ amplitudes in the LLA (including disconnected contributions):

$$T^{(1)} = \tag{1.4}$$

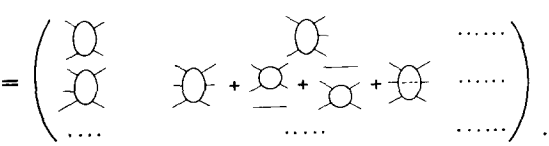

Taking for each $n \to m$ amplitude the sum of all its energy discontinuities (for the $2 \to 3$ process $1 + 2 \to a + b + c$, for example there are the variables s, s_{ab}, s_{bc}, and

s_{ac} and, correspondingly, four discontinuity equations), the results of I can be summarized in the following matrix equation:

$$\Delta T^{(1)} = \frac{1}{2i}(T^{(1)} - T^{(1)+}) = \tfrac{1}{2} T^{(1)} T^{(1)+}_{\text{odd signature}} . \tag{1.5}$$

The restriction on the r.h.s. of (1.1)–(1.3) and (1.5) signalizes that s-channel unitarity is satisfied only in a limited sense, and we have to go beyond the LLA for obtaining complete unitarity.

In order to improve the LLA we make the ansatz (again using matrix notation):

$$T = \sum_{n=1}^{\infty} T^{(n)}, \tag{1.6}$$

where the first term on the r.h.s., $T^{(1)}$, is just the LLA and the remaining terms $T^{(n)}$ have to be calculated from the requirement that unitarity is fully satisfied:

$$\Delta T = \frac{1}{2i}(T - T^{+}) = \tfrac{1}{2} T T^{+} . \tag{1.7}$$

Eq. (1.6) is an expansion in powers of the coupling constant g^2. In any given order of perturbation theory the high-energy behavior for, say, the $2 \to 2$ amplitude comes in the form:

$$g^{2n} s \left[(\ln s)^{n-1} f_{n-1}(t) + (\ln s)^{n-2} f_{n-2}(t) + \cdots + f_0(t) \right] + O(s^0) + O(s^{-1}) + \cdots . \tag{1.8}$$

The LLA then represents the sum of the first term on the r.h.s. of this expansion:

$$\text{LLA} = \sum_n g^{2n} s (\ln s)^{n-1} f_{n-1}(t) . \tag{1.9}$$

The next order correction in (1.6), $T^{(2)}$, consists of the $f_{n-2}(t)$, $T^{(3)}$ is the sum of the $f_{n-3}(t)$, etc. Equivalently, $T^{(2)}$ has one more power of g^2 than $T^{(1)}$, $T^{(3)}$ has two more powers of g^2 and so on.

For the computation of $T^{(2)}, T^{(3)} \ldots$, we will, as we did in I, again make full use of the analytic structure of multiparticle amplitudes in the Regge region, i.e., employ both t- and s-channel unitarity. This does, *a priori*, not guarantee that we will find all pieces of $f_{n-2}, f_{n-3}, \ldots$, in (1.8). We rather expect that we will find only that subset of all the non-leading terms which are necessary to just satisfy unitarity. The results of our calculation should, therefore, be regarded as the *minimal* subset of terms in the perturbation expansion that have to be taken into account in order to obtain a reliable high-energy theory. We can, however, not yet rule out the

possibility that this is still not enough: in this case our result would be the first-order approximation to the exact solution. An answer to this question can be given at earliest, when we know the *sum* of all terms which we are going to determine in the following.

Although the construction of a unitary high-energy description of massive Yang-Mills theory is of interest by itself, the most fascinating problem is certainly the high-energy behavior of pure Yang-Mills theories, in particular, QCD. We, therefore, shall try to use our calculations as an intermediate step towards approaching massless vector theories. The question of whether and how QCD in the confining phase can be reached in the zero-mass limit of a Higgs model has not been answered yet. In the context of our calculations this question represents itself in the following form. Within the approximation we are using, the S-matrix only depends on the gauge coupling g and the mass M of the vector particle, but not on the Higgs parameters (the mass of the scalar particle, the Higgs self-coupling) separately. It is, therefore, first necessary to show that the limit $M \to 0$ exists and is finite. Whether we then can hope to be in the confining phase of QCD or not can be shown only by performing the summation of all the terms in the expansion (1.6): as we have outlined elsewhere [5], there is a parameter $\langle b^2 \rangle$ which measures the extension of the scattering hadron transverse to its direction of flight and can be used as an indication of to what extent the present approach has a chance to "confine" the wee partons inside the hadrons.

In the present paper we shall construct the first term beyond the LLA in the expansion (1.6), $T^{(2)}$. Since this approximation contains the vacuum exchange channel, we also address ourselves to the $M \to 0$ limit: replacing the external particles by $q\bar{q}$ bound states, we shall show that the zero-mass limit exists order by order in perturbation theory. In view of future work we also present a generalization of this proof to larger classes of diagrams (subsets of $T^{(3)}, T^{(4)}, \ldots$). This will help us (as we shall show elsewhere [6]) to formulate a new technique for summing all diagrams. In sect. 2 we begin with a few general definitions. Sects. 3 and 4 contain the calculation of $T^{(2)}_{2\to 3}$ and $T^{(2)}_{2\to 4}$, respectively. In sect. 5 we present a study of the zero-mass limit, and sect. 6 contains a brief summary and an outlook on future parts of our program. A few details of our calculations are put into an appendix.

2. Definitions

We begin with a somewhat more detailed outline of how the elements of the matrix $T^{(2)}$ will be constructed. The defining equation is:

$$\Delta T^{(2)} = \frac{1}{2i}(T^{(2)} - T^{(2)+}) = \tfrac{1}{2} T^{(1)} T^{(1)+}_{\text{even signature}}, \tag{2.1}$$

where on the r.h.s. each matrix element has one or more even signature exchange channels [otherwise we would be back at (1.5)]. The presence of even signature

implies that $T^{(2)}$ will be down by one power of g^2 compared with $T^{(1)}$: the signature phase factor $e^{-i\pi j} + \tau$ with $j = 1 + O(g^2)$ when expanded in powers of g^2, starts with -2 for odd ($\tau = -$) signature but with $O(g^2)$ for even ($\tau = +$) signature. Eq. (2.1) can be read as an equation for energy discontinuities, for example for the element $T^{(2)}_{2\to 3}$,

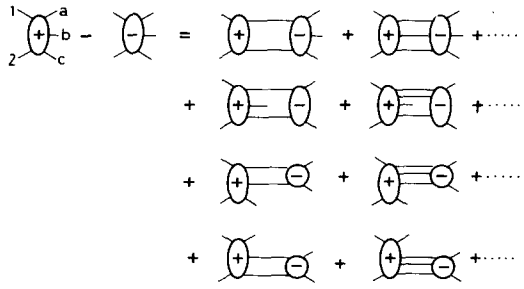

(2.2)

On the r.h.s. the first line is the discontinuity in the total energy s, the second line represents the discontinuity in the subenergy s_{ac}, the third line in s_{ab}, and the last line in s_{bc}. In order to write also the l.h.s. as a sum of discontinuities, we have to make use of a general feature of the $2\to 3$ amplitude in the double-Regge limit [cf. eqs. (2.6), (2.7) and fig. 5a of I]. In this limit, $T_{2\to 3}$ can be written as the sum of two terms:

$$T_{2\to 3}(s, s_{ab}, s_{bc}) = T_{ab}(s, s_{ab}) + T_{bc}(s, s_{bc}) \tag{2.3}$$

(we suppress the dependence on other variables than energies), and each of the terms on the r.h.s. satisfies a double dispersion relation with right- and left-hand cuts. It follows from the definition of the double-Regge limit,

$$s, s_{ab}, s_{bc} \to \infty, \qquad s_{ab}/s, s_{bc}/s \to 0,$$

$$t_1, t_2, \eta = s_{ab} \cdot s_{bc}/s \text{ fixed}, \tag{2.4}$$

that several energy variables become asymptotically equal and cannot be distinguished from each other:

$$s_{ac} = (p_a + p_c)^2 \approx s,$$

$$s_{1\bar{b}} = (p_1 - p_b)^2 \approx -s_{ab},$$

$$s_{2\bar{b}} = (p_2 - p_b)^2 \approx -s_{bc}. \tag{2.5}$$

On the r.h.s. of eq. (2.3) the term T_{ab} contains, therefore, a piece which depends on s and s_{ab} and another one which depends on s_{ac} and $s_{1\bar{b}}$. Similarly, the dependence

of T_{bc} is either on (s, s_{bc}) or $(s_{ac}, s_{2\bar{b}})$. The l.h.s. of eq. (2.2) can be written as:

$$\begin{aligned}\Delta T_{2\to 3} &= \frac{1}{2i}\left(T_{2\to 3}(\text{all energies} + i\varepsilon) - T_{2\to 3}(\text{all energies} - i\varepsilon)\right)\\ &= \Delta_{abc}\left(T_{ab}(s, s_{ab} - i\varepsilon) + T_{bc}(s, s_{bc} - i\varepsilon)\right)\\ &\quad + \Delta_{ac}\left(T_{ab}(s, s_{ab}) + T_{bc}(s, s_{bc})\right)\\ &\quad + \Delta_{ab}T_{ab}(s + i\varepsilon, s_{ab}) + \Delta_{bc}T_{bc}(s + i\varepsilon, s_{bc}) \qquad (2.6)\end{aligned}$$

(here Δ_{abc} denotes the discontinuity across the total energy). The four terms in (2.6) can be identified with the r.h.s. of (2.2): this equation will be satisfied if the sum of the discontinuities in s_{abc} and s_{ac} equals the sum of the first two lines on the r.h.s. of (2.2), and the s_{ab} and s_{bc} discontinuities are identical with the third and fourth line of (2.2), respectively (note that we do not require to compare the s_{abc} and s_{ac} discontinuities separately: since these two variables become indistinguishable, we cannot separate their discontinuities). In the same way, the other elements of the matrix equation (2.1) contain sums of single discontinuities of the $n\to m$ amplitudes.

This then leads to the following method of computing $T^{(2)}$. From the product $T^{(1)}T^{(1)+}$ on the r.h.s of (2.1) we calculate the various single discontinuities of each element of $T^{(2)}$, and we then search for the amplitude which correctly reproduces the sum of the discontinuities on the r.h.s. of eq. (2.1). For this it will be convenient to use that representation of $T_{n\to m}$ which exhibits the full analytic structure. A list of these representations (which we have already used in I) is given in table 1, together with the form of the signature factors. In the case of the $2\to 3$ amplitude one recognizes the two terms (2.3), and a similar decomposition can be read off for the $2\to 4$ and $3\to 3$ amplitudes (there is a slight complication concerning the last two terms of these amplitudes which we shall discuss a little later). In the following two sections we shall illustrate how the partial wave functions $F_{\dots}$ (or combinations of them) can be constructed by evaluating single discontinuities. The representations of table 1 then allow us to find the full amplitudes.

The result of our calculations will be that the elements of $T^{(2)}$ come in form of reggeon calculus [7], i.e., each partial wave $F_{\dots}$ can be described in a diagrammatic way (as was already the case for $T^{(1)}$). Once we know the partial waves it is, however, useful to combine the various terms in the representations of table 1 into one single expression. As an example, we consider the $2\to 3$ amplitude. The energy factors of $T_{2\to 3}$ can be written as:

$$\begin{aligned}s^{j_2}s_{ab}^{j_1-j_2} &= s s_{ab}^{j_1-1} s_{bc}^{j_2-1}\eta^{-(j_2-1)}\\ &= s s_{ab}^{j_1-1} s_{bc}^{j_2-1}\left(1 + O(g^2\eta)\right), \qquad (2.7)\end{aligned}$$

where we have used the fact that the singularities in j are always of the form $j_{sing} = 1 + O(g^2)$. According to (2.4) η is finite in the double-Regge limit, and we can safely neglect terms of the order $O(g^2 \ln \eta)$. Now it is possible to combine the

TABLE 1
Analytic representations of $T_{2\to2}$, $T_{2\to3}$, $T_{2\to4}$, and $T_{3\to3}$

$$T_{2\to2} = \frac{1}{2\pi i}\int \mathrm{d}j\, s^j \xi_j F(j,t)$$

$$T_{2\to3} = \frac{1}{(2\pi i)^2}\int \mathrm{d}j_1\,\mathrm{d}j_2 [s^{j_1} s_{\mathrm{b_c}}^{j_2-j_1}\xi_{j_1}\xi_{j_2 j_1} F_{\mathrm{L}}(j_1,j_2,t,t_2,\eta) + s^{j_2} s_{\mathrm{ab}}^{j_1-j_2}\xi_{j_2}\xi_{j_1 j_2} F_{\mathrm{R}}(j_1,j_2,t_1,t_2,\eta)]$$

$$\begin{aligned} T_{2\to4} = \frac{1}{(2\pi i)^3}\int \mathrm{d}j_1\,\mathrm{d}j_2\,\mathrm{d}j_3 [& s^{j_1} s_{\mathrm{bcd}}^{j_2-j_1} s_{\mathrm{cd}}^{j_3-j_2}\xi_{j_1}\xi_{j_2 j_1}\xi_{j_3 j_2} F_{\mathrm{LL}} + s^{j_2} s_{\mathrm{ab}}^{j_1-j_2} s_{\mathrm{cd}}^{j_3-j_2}\xi_{j_2}\xi_{j_1 j_2}\xi_{j_3 j_2} F_{\mathrm{RL}} \\ & + s^{j_3} s_{\mathrm{abc}}^{j_2-j_3} s_{\mathrm{ab}}^{j_1-j_2}\xi_{j_3}\xi_{j_2 j_3}\xi_{j_1 j_2} F_{\mathrm{RR}} + s^{j_3} s_{\mathrm{abc}}^{j_1-j_3} s_{\mathrm{bc}}^{j_2-j_1}\xi_{j_3}\xi_{j_1 j_3}\xi_{j_2 j_1} F_{\mathrm{LR}}^{(1)} \\ & + s^{j_1} s_{\mathrm{bcd}}^{j_3-j_1} s_{\mathrm{bc}}^{j_2-j_3}\xi_{j_1}\xi_{j_3 j_1}\xi_{j_2 j_3} F_{\mathrm{LR}}^{(2)}] \end{aligned}$$

$$\begin{aligned} T_{3\to3} = \frac{1}{(2\pi i)^3}\int \mathrm{d}j_1\,\mathrm{d}j_2\,\mathrm{d}j_3 [& s^{j_1} s_{\mathrm{b2}}^{j_2-j_1} s_{\mathrm{cd}}^{j_3-j_2}\xi_{j_1}\xi_{j_2 j_1}\xi_{j_3 j_2} F_{\mathrm{LL}} + s^{j_2} s_{1\bar{\mathrm{b}}}^{j_1-j_2} s_{\mathrm{cd}}^{j_3-j_2}\xi_{j_2}\xi_{j_1 j_2}\xi_{j_3 j_2} F_{\mathrm{RL}} \\ & + s^{j_3} s_{1\bar{\mathrm{b}}}^{j_1-j_2} s_{\mathrm{ac}}^{j_2-j_3}\xi_{j_3}\xi_{j_1 j_2}\xi_{j_2 j_3} F_{\mathrm{RR}} + s^{j_1+j_3-j_2} s_{\mathrm{ac}}^{j_2-j_3} s_{\mathrm{b2}}^{j_2-j_1}\xi_{j_2 j_3}\xi_{j_2 j_1}\xi_{j_1+j_3-j_2} F_{\mathrm{LR}}^{(1)} \\ & + s_{\mathrm{ac}}^{j_1} s_{\mathrm{b2}}^{j_3} s^{j_2-j_1-j_3}\bar{\mathrm{I}}_{\mathrm{ac}}^{-1}\xi_{j_1}\xi_{j_3}\xi_{j_2-j_1-j_3} F_{\mathrm{LR}}^{(2)}] \end{aligned}$$

$$\xi_j = \frac{\mathrm{e}^{-i\pi j}+\tau}{\sin\pi j}$$

$$\xi_{j_1 j_2} = \frac{\mathrm{e}^{-i\pi(j_1-j_2)}+\tau_1\tau_2}{\sin\pi(j_1-j_2)}$$

$$\xi_{j_1+j_3-j_2} = \frac{\mathrm{e}^{-i\pi(j_1+j_3-j_2)}+\tau_1\tau_2\tau_3}{\sin\pi(j_1+j_3-j_2)}$$

signature factors and partial waves, e.g., for the two cases $(\tau_1,\tau_2)=(-,-)$ and $(+,+)$:

$$T_{2\to3}(-,-) = \frac{2s}{(2\pi i)^2}\int \mathrm{d}\omega_1\,\mathrm{d}\omega_2 s_{\mathrm{ab}}^{\omega_1} s_{\mathrm{bc}}^{\omega_2}\left[\frac{F_{\mathrm{L}}}{\omega_1(\omega_2-\omega_1)}+\frac{F_{\mathrm{R}}}{\omega_2(\omega_1-\omega_2)}\right]\frac{2}{\pi^2}, \tag{2.8}$$

$$T_{2\to3}(+,+) = \frac{2s\pi i}{(2\pi i)^2}\int \mathrm{d}\omega_1\,\mathrm{d}\omega_2 s_{\mathrm{ab}}^{\omega_1} s_{\mathrm{bc}}^{\omega_2}\left[\frac{F_{\mathrm{L}}}{\omega_2-\omega_1}+\frac{F_{\mathrm{R}}}{\omega_1-\omega_2}\right]\frac{-1}{\pi^2} \tag{2.9}$$

(here $\omega_i = j_i - 1$). The first case belongs to $T^{(1)}$, and in I it was shown that the square bracket term takes the simple form (fig. 1a):

$$\begin{aligned} & \frac{2}{\pi^2}\left[\frac{F_{\mathrm{L}}}{\omega_1(\omega_2-\omega_1)}+\frac{F_{\mathrm{R}}}{\omega_2(\omega_1-\omega_2)}\right] \\ & \quad = [gH_{\mathrm{vv}}]\frac{1}{\omega_1-\alpha(t_1)+1}\frac{1}{t_1-M^2}[g\Gamma]\frac{1}{\omega_2-\alpha(t_2)+1}\frac{1}{t_2-M^2}[gH_{\mathrm{vv}}] \\ & \qquad \cdot \text{group structure fig. 1b}. \end{aligned} \tag{2.10}$$

A comparison of the r.h.s. of (2.10) and fig. 1a suggests the following diagrammatic rules for the Mellin transform of the scattering amplitude, i.e., the term in square brackets on the r.h.s. of (2.8): each reggeon line with momentum $k_\perp$ has a propagator

$$\left[t - M^2\right]^{-1}\left[\omega - \alpha(t) + 1\right]^{-1}, \qquad \text{where } t = -k_\perp^2 \tag{2.11}$$

[where $\alpha(t)$ is the trajectory function, given in eqs. (4.6) and (4.9) of I]; for the production vertex the three-component vector [eqs. (3.6) and (3.7) of I]

$$g\Gamma(q_1, -q_2)\,; \tag{2.12}$$

for the coupling of a reggeon to external particles the matrix H_{vv} or H_{vs} [eqs. (3.2) and (3.3) of I]. For the group structure we draw a separate diagram (fig. 1b), in which each vertex has a tensor ε_{abc} (or δ_{ab} if one of the particles is a Higgs scalar). In the following we shall find that for the case of eq. (2.9) the term in square brackets also has such a simple form and can be described by these diagrammatic rules (with some new elements that we will derive), and this appealing situation holds for each signature configuration of all $T^{(2)}_{n\to m}$.

3. Construction of $T^{(2)}_{2\to 2}$ and $T^{(2)}_{2\to 3}$

The first element of the matrix equation (2.1) is (fig. 2a):

$$\text{disc}_s\, T^{(2)}_{2\to 2} = \tfrac{1}{2}\sum_n \int \mathrm{d}\Omega_n \left|T_{2\to n}\right|^2_{\text{even signature}}. \tag{3.1}$$

In order to identify the r.h.s. of this equation with fig. 2a, we define the following rules: for each momentum and angular momentum loop we put

$$\int \frac{\mathrm{d}^2 k_\perp}{(2\pi)^3} \int \frac{\mathrm{d}\omega}{2\pi i}\,, \tag{3.2}$$

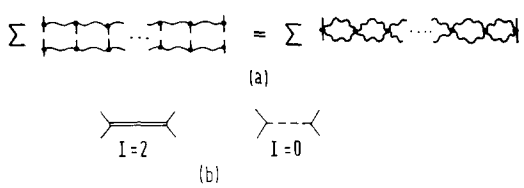

Fig. 2. (a) Construction of $T^{(2)}_{2\to 2}$ from its s discontinuity. (b) The group weight diagrams for $I = 2$ and $I = 0$ exchange. The corresponding tensors are the projection operators P_2 and P_0, defined in eq. (4.3) of I.

where $-k_\perp^2 = t$ is the momentum transfer and $j = \omega + 1$. The quartic reggeon vertex in fig. 2a which results from squaring the production vertex has been derived before (ref. [8] and I), but in order to make this paper as self-contained as possible we present in the appendix a summary of all those rules which one needs for deriving the momentum or helicity structure of vertices. For the group structure we decompose the tensor which arises from squaring the production vertex into projection operators with definite isospin ($I = 0, 1, 2$) [cf. eqs. (4.3)–(4.7) of I]: $I = 0$ or 2 belongs to even signature exchange since it is symmetric, whereas $I = 1$ is antisymmetric and belongs to odd signature. As a result of this, the quartic reggeon vertex comes with a group weight factor (-2 for $I = 0$, -1 for $I = 1$, $+1$ for $I = 2$), and the full diagram is proportional to the projection operator P_0, P_1, or P_2. For this part of the diagram we draw a separate graph: our notation for P_0 and P_2 is shown in fig. 2b (P_1 belongs to odd signature and is defined in I). With all these conventions eq. (3.1) can be written

$$\mathrm{disc}_s\, T^{(2)}_{2\to 2} = 2\pi \cdot \text{fig. 2a} \cdot \text{fig. 2b} \tag{3.3}$$

(note the factor 2π: applying our rules to fig. 2a, we obtain the partial wave of $T^{(2)}_{2\to 2}$ up to this factor 2π). From table 1 we then find the full amplitude $T^{(2)}_{2\to 2}$ with even signature exchange:

$$T^{(2)}_{2\to 2} = 2\pi i s \int \frac{\mathrm{d}\omega}{2\pi i} s^\omega F_{2\to 2}(\omega, t)\,,$$

$$F_{2\to 2} = \text{fig. 2a} \cdot \text{fig. 2b}\,. \tag{3.4}$$

For the vacuum exchange channel, the leading j-plane singularity has been shown [2, 3] to be a fixed cut to the right of $j = 1$, whereas in the $I = 2$ channel the leading singularity is the two-reggeon cut. Although $T^{(2)}$ does not belong to the LLA (in the sense we have defined it), (3.15) is often referred to as the leading logarithmic approximation for the pomeron (or the $I = 2$ exchange): this is because the vacuum exchange channel was not contained in the LLA, $T^{(1)}$, and $T^{(2)}$ is the lowest approximation where it appears. It has also been calculated by conventional methods, i.e., by extracting leading powers of lns from Feynmann amplitudes [9].

Next we come to $T^{(2)}_{2\to 3}$. That part of the product $T^{(1)}T^{(1)+}$ which has odd signature (or $I = 1$) in both t-channels belongs to $T^{(1)}$ [see eq. (1.5)]. The remaining signature configurations are $(\tau_1, \tau_2) = (+, +)$, $(+, -)$, and $(-, +)$. We begin with the $(+, +)$ configuration. The r.h.s. of (2.1) determines the discontinuities in s and s_{ac}:

$$\Delta_{abc} T^{(2)}_{2\to 3}(+, +) = 2\pi \cdot \text{fig. 3a} \cdot \text{group weight}\,, \tag{3.5}$$

$$\Delta_{ac} T^{(2)}_{2\to 3}(+, +) = 2\pi \cdot \text{fig. 3b} \cdot \text{group weight}\,, \tag{3.6}$$

but there is no equation for the s_{ab} or s_{bc} discontinuities. The signature requirement allows only for $I = 0$ or 2 in the t-channels, and the corresponding group diagrams are shown in fig. 3c. For the diagrammatic rules we use the same conventions as before: it is then easy to see that figs. 3a, b lead to the same expression:

$$\Delta_{abc} T^{(2)}_{2\to 3}(+,+) = \Delta_{ac} T^{(2)}_{2\to 3}(+,+) . \tag{3.7}$$

In order to find from table 1 the discontinuities in s and s_{ac}, we note that since the two variables s and s_{ac} become indistinguishable in the double-Regge limit (2.4) the variable s in table 1 can be either s or s_{ac}, and only the sum of both discontinuities can be calculated safely:

$$(\Delta_{abc} + \Delta_{ac}) \xi_{j_2 j_1} \xi_{j_1} s^{j_1} s_{bc}^{j_2 - j_1} = -\xi_{j_2 j_1} s^{j_1} s_{bc}^{j_2 - j_1} . \tag{3.8}$$

This is consistent with the idea that the signatured amplitude is a combination of the four crossing related processes $1 + 2 \to a + b + c$, $\bar{a} + 2 \to \bar{1} + b + c$, $1 + \bar{c} \to a + b + \bar{2}$, and $\bar{a} + \bar{c} \to \bar{1} + b + \bar{2}$. From this one would interpret the energy and phase factors of (3.8) as

$$\begin{aligned} &\frac{e^{-i\pi(j_2 - j_1)} + \tau_1 \tau_2}{\sin \pi (j_2 - j_1)} \frac{e^{-i\pi j_1} + \tau_1}{\sin \pi j_1} s^{j_1} s_{bc}^{j_2 - j_1} \\ &\quad = [\sin \pi (j_2 - j_1)]^{-1} [\sin \pi j_1]^{-1} \Big[e^{-i\pi(j_2 - j_1)} e^{-i\pi j_1} s^{j_1} s_{bc}^{j_2 - j_1} \\ &\qquad + \tau_1 e^{-i\pi(j_2 - j_1)} (-s_{\bar{a}2})^{j_1} s_{bc}^{j_2 - j_1} + \tau_2 (-s_{\bar{c}1})^{j_1} \\ &\qquad \times (-s_{\bar{b}2})^{j_2 - j_1} + \tau_1 \tau_2 e^{-i\pi j_1} s_{ac}^{j_1} (-s_{\bar{b}2})^{j_2 - j_1} \Big] . \end{aligned} \tag{3.9}$$

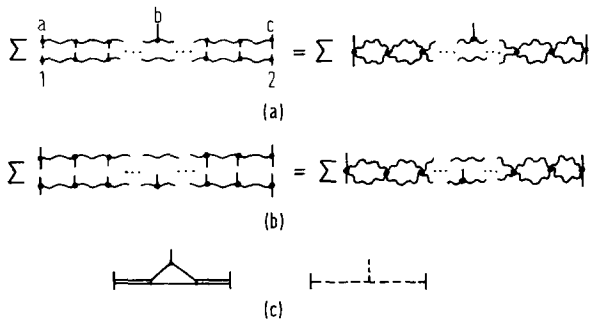

Fig. 3. Construction of $T^{(2)}_{2\to 3}$ with signature $(\tau_1, \tau_2) = (+,+)$: (a) the s discontinuity; (b) the s_{ac} discontinuity; (c) two possible weight diagrams.

The discontinuities in s and s_{ac} come from the first and fourth term, respectively, and their sum agrees with (3.8). For more complicated amplitudes than $T_{2\to3}$, however, an interpretation à la (3.9) is presumably too naive, i.e., it will be impossible to compute discontinuities in variables such as s and s_{ac} separately. It is then only the sum of discontinuities which can be defined. We thus have

$$(\Delta_{abc}+\Delta_{ac})T^{(2)}_{2\to3}=\frac{-2\pi s}{(2\pi i)^2}\int d\omega_1\, d\omega_2 s_{ab}^{\omega_1}s_{bc}^{\omega_2}\frac{1}{\pi^2}\left[\frac{F_L-F_R}{\omega_2-\omega_1}\right]. \tag{3.10}$$

Together with (3.5) and (3.6) this leads to the result:

$$\frac{1}{\pi^2}\left[\frac{F_L-F_R}{\omega_2-\omega_1}\right]=-\text{fig. 3a}\cdot\text{group weight}. \tag{3.11}$$

The full amplitude is

$$T^{(2)}_{2\to3}(+,+)=\frac{-2\pi is}{(2\pi i)^2}\int d\omega_1\, d\omega_2 s_{ab}^{\omega_1}s_{bc}^{\omega_2}\frac{1}{\pi^2}\frac{F_L-F_R}{\omega_2-\omega_1}$$

$$=\frac{2\pi is}{(2\pi i)^2}\int d\omega_1\, d\omega_2 s_{ab}^{\omega_1}s_{bc}^{\omega_2}\cdot\text{fig. 3a}\cdot\text{group weight}. \tag{3.12}$$

A few words should be said about the s_{ab} and s_{bc} discontinuities. The use of eq. (2.1) enabled us to find an expression for the combination of partial waves $(F_L-F_R)/(\omega_2-\omega_1)$, but not F_L and F_R separately. This was sufficient, since the full amplitude (3.11) was found to be proportional to its discontinuity in s (or s_{ac}). Nevertheless, one may ask what the partial waves F_L and F_R are. Counting powers of g^2, one sees that the s_{ab} (s_{bc}) discontinuity comes at a later stage of our scheme, namely from the product $T^{(2)}T^{(1)+}$ which, in our definition, is part of $T^{(3)}$. The diagrams for F_L and F_R are shown in figs. 4a and b. In order that these results are in agreement with the expression for $(F_L-F_R)/(\omega_2-\omega_1)$ (fig. 3a), the following equation must be true:

$$2\pi^2\cdot\text{fig. 3a}=2\pi^2\frac{\text{fig. 4a}-\text{fig. 4b}}{\omega_2-\omega_1} \tag{3.13}$$

(we leave out the group structure diagrams). We have checked this equation in lowest non-trivial order perturbation theory, g^7, and found that it is satisfied. This indicates that the bootstrap equation of fig. 5a (see also fig. 36a of I) which was first found by Lipatov et al. [2] is only *one* example of a much larger set of identities which are fulfilled by $T^{(1)}$ and $T^{(2)}$. Other examples are obtained from the requirement that, for $T^{(1)}$, the calculation of double discontinuities must lead to the

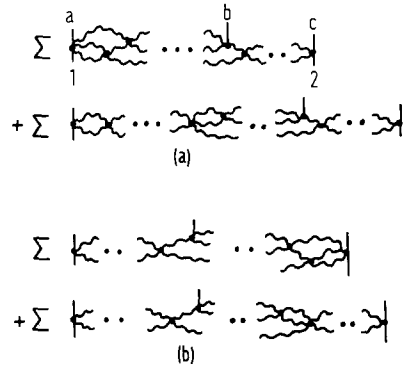

Fig. 4. Reggeon diagrams for the partial waves (a) F_L and (b) F_R of $T^{(2)}_{2\to 3}$ with signature (+, +).

same answer as single discontinuities, e.g., (fig. 5b)

$$\Delta_{ab} T^{(1)}_{2\to 3} = -\frac{2}{\pi\omega_2}(\Delta_{abc} + \Delta_{ac})\,\Delta_{ab} T^{(1)}_{2\to 3}, \tag{3.14}$$

$$\Delta_{bc} T^{(1)}_{2\to 3} = -\frac{2}{\pi\omega_1}(\Delta_{abc} + \Delta_{ac})\,\Delta_{bc} T^{(1)}_{2\to 3}. \tag{3.15}$$

We have checked these equations again in lowest non-trivial order in g and found that they are satisfied. Identities of this kind will also play an important role in the future part of our program.

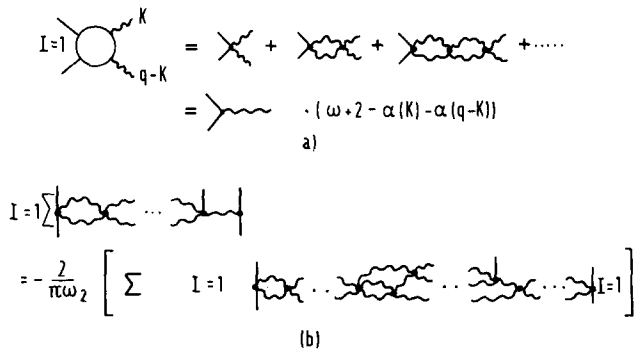

Fig. 5. (a) Bootstrap equation for the $I = 1$ exchange amplitude (from ref. [2]); (b) bootstrap equation, (3.14).

Next we come to the signature combination $(\tau_1, \tau_2) = (-, +)$. The product $T^{(1)}T^{(1)+}$ defines the discontinuities in s, s_{ac}, and s_{bc}:

$$\Delta_{abc} T^{(2)}_{2\to 3}(-, +) = 2\pi \cdot \text{fig. 6a} \cdot \text{group weight}, \tag{3.16}$$

$$\Delta_{ac} T^{(2)}_{2\to 3}(-, +) = 2\pi \cdot \text{fig. 6b} \cdot \text{group weight}, \tag{3.17}$$

$$\Delta_{bc} T^{(2)}_{2\to 3}(-, +) = 2\pi \cdot \text{fig. 6c} \cdot \text{group weight}. \tag{3.18}$$

For the construction of the production vertex in fig. 6c we refer to the appendix. When going in figs. 6a, b from the l.h.s. to the r.h.s. we use the bootstrap equation, fig. 5a. The signature requirements imply that the t_1-channel has $I = 1$ exchange, the t_2-channel either $I = 0$ or $I = 2$. Since the group structure diagram is now antisymmetric when "twisting" the t_1-channel, figs. 6a, b are identical up to an overall minus sign:

$$\Delta_{abc} T^{(2)}_{2\to 3}(-, +) = -\Delta_{ac} T^{(2)}_{2\to 3}(-, +). \tag{3.19}$$

The sum of these two discontinuities therefore cancels and gives no information about the amplitudes we are looking for. From table 1 we see that, to leading order g^2, the amplitude $T^{(2)}_{2\to 3}(-, +)$ is given by F_L only: since both partial wave functions F_L and F_R must be calculable from double discontinuities, they are of the same order in g^2, namely $g^3 f(g^2/\omega)$, and the signature factors in front of F_R have

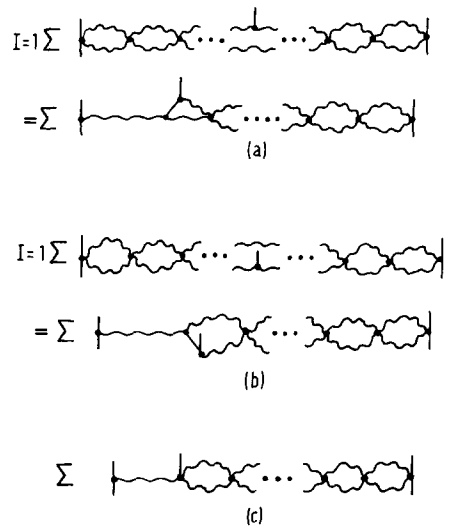

Fig. 6. Construction of $T^{(2)}_{2\to 3}$ with signature $(-, +)$: (a) the s discontinuity; (b) the s_{ac} discontinuity; (c) the s_{bc} discontinuity.

one more power of g^2 than those in front of F_L. This implies that $T^{(2)}_{2\to3}(-,+)$ is determined by its s_{bc} discontinuity:

$$T^{(2)}_{2\to3}(-,+) = \frac{-is}{(2\pi i)^2}\int d\omega_1\, d\omega_2 s^{\omega_1}_{ab} s^{\omega_2}_{bc} \frac{2}{\pi}\frac{F_L}{\omega_1}$$

$$= i\Delta_{bc} T^{(2)}_{2\to3}(-,+), \tag{3.20}$$

$$-\frac{2}{\pi\omega_1}F_L = 2\pi\cdot\text{fig. 6c}\cdot\text{group weight}. \tag{3.21}$$

When we calculate the s and s_{ac} discontinuities, both partial wave functions participate, but their sum is of higher order in g^2 than the s_{bc} discontinuity. Within the approximation we are using, the s and s_{ac} discontinuities, therefore, cancel, in agreement with (3.19). As a result, eq. (2.1) will be satisfied if we put

$$T^{(2)}_{2\to3}(-,+) = \frac{2\pi is}{(2\pi i)^2}\int d\omega_1\, d\omega_2 s^{\omega_1}_{ab} s^{\omega_2}_{bc}\cdot\text{fig. 6c}\cdot\text{group weight}. \tag{3.22}$$

4. Construction of $T^{(2)}_{2\to4}$, $T^{(2)}_{3\to3}$, and generalization to $T^{(2)}_{n\to m}$

The five-point amplitudes which we have constructed in sect. 3 do not yet exhibit the full complexity of the analytic structure of multiparticle amplitudes. In order to be able to write down the general amplitude $T^{(2)}_{n\to m}$ we have to go one step further and consider the six-point amplitudes $T^{(2)}_{2\to4}$ and $T^{(2)}_{3\to3}$ (fig. 7). In the multi-Regge limit,

$$s, s_{abc}, s_{bcd}, s_{ab}, s_{bc}, s_{cd} \to \infty,$$

$$s_{ab}/s_{abc}, s_{bc}/s_{abc}, s_{bc}/s_{bcd}, s_{cd}/s_{bcd}, s_{abc}/s, s_{bcd}/s \to 0,$$

$$t_1, t_2, t_3 \text{ fixed}, \qquad \eta_b = \frac{s_{ab}s_{bc}}{s_{abc}}, \eta_c = \frac{s_{bc}s_{cd}}{s_{bcd}} \text{ fixed}, \tag{4.1}$$

these amplitudes decay into several pieces, each of which has a simple analytic structure and satisfies a multiple dispersion relation with right- and left-hand singularities. The representations of table 1 (which originally have been derived for amplitudes containing only Regge poles but no cuts) indicate that there are five such terms, and figs. 7a, b illustrate their discontinuity content in the physical region (right-hand singularities): each dotted lines denotes an energy variable $s_{ij\ldots}$ for which the amplitude has a non-zero discontinuity, and in the representation of table 1 there is a corresponding factor $s^{\text{power}}_{ij\ldots}$. The left-hand cut structure follows

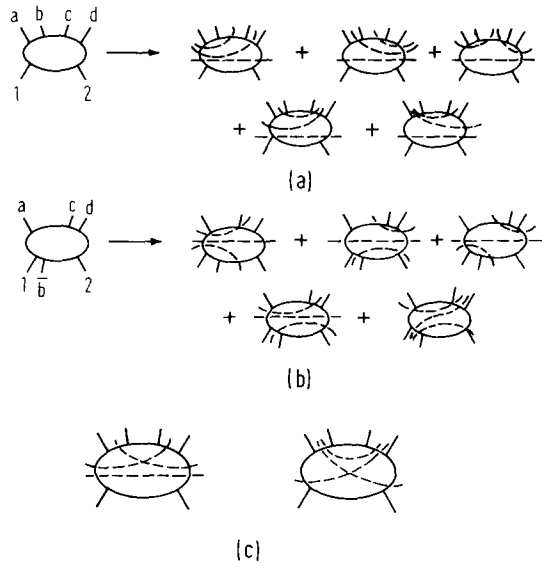

Fig. 7. The analytic structure of the two six-point amplitudes: (a) the five planar terms of the $2\to4$ amplitudes; (b) the five planar terms of the $3\to3$ amplitude; (c) two contributions to $T_{2\to4}$ which are included in the last two terms of the representation of table 1.

from the fact that the fully signatured $2\to4$ and $3\to3$ amplitudes are connected by analytic continuation and crossing, such that they are even or odd under a twist of a t-channel. For constructing $T^{(2)}_{2\to4}$ or $T^{(2)}_{3\to3}$ it is, therefore, necessary to consider simultaneously the eight amplitudes shown in fig. 8. Each of them has its five terms (fig. 7a and b): for the first three it is obvious that analytic continuation of $T^{(2)}_{2\to4}$ leads to the corresponding terms of $T^{(2)}_{3\to3}$. This can be made explicit by rewriting energy and phase factors in the same way as we did in (3.9):

$$\begin{aligned}
\xi_{j_1}\xi_{j_2 j_1}\xi_{j_3 j_2} s^{j_1} s^{j_2-j_1}_{\mathrm{bcd}} s^{j_3-j_2}_{\mathrm{cd}} = {} & \left[\sin\pi j_1\right]^{-1}\left[\sin\pi(j_2-j_1)\right]^{-1}\left[\sin\pi(j_3-j_2)\right]^{-1} \\
& \times\Big[\mathrm{e}^{-i\pi j_1}\,\mathrm{e}^{-i\pi(j_2-j_1)}\,\mathrm{e}^{-i\pi(j_3-j_2)} s^{j_1} s^{j_2-j_1}_{\mathrm{bcd}} s^{j_3-j_2}_{\mathrm{cd}} \\
& + \tau_1\,\mathrm{e}^{-i\pi(j_2-j_1)}\,\mathrm{e}^{-i\pi(j_3-j_2)} |s^{j_1}_{\bar{\mathrm{a}}2}|\, s^{j_2-j_1}_{\mathrm{bcd}} s^{j_3-j_2}_{\mathrm{cd}} \\
& + \tau_2\,\mathrm{e}^{-i\pi(j_3-j_2)} |s^{j_1}_{\mathrm{a}\bar{\mathrm{b}}2}|\, |s^{j_2-j_1}_{\mathrm{bcd}}|\, |s^{j_3-j_2}_{\mathrm{cd}}| + \tau_3 |s^{j_1}_{1\bar{\mathrm{d}}}|\, |s^{j_2-j_1}_{\mathrm{bc}\bar{2}}|\, |s^{j_3-j_2}_{\mathrm{c}\bar{2}}| \\
& + \tau_1\tau_2\,\mathrm{e}^{-i\pi j_1}\,\mathrm{e}^{-i\pi(j_3-j_2)} s^{j_1}_{1\bar{\mathrm{b}}2}\, |s^{j_2-j_1}_{\mathrm{bcd}}|\, s^{j_3-j_2}_{\mathrm{cd}} \\
& + \tau_2\tau_3\,\mathrm{e}^{-i\pi j_1}\,\mathrm{e}^{-i\pi(j_2-j_1)} s^{j_1}_{1\bar{\mathrm{c}}2} s^{j_2-j_1}_{\mathrm{b}\bar{\mathrm{c}}\mathrm{d}} |s^{j_3-j_2}_{\bar{\mathrm{c}}2}| \\
& + \tau_1\tau_3\,\mathrm{e}^{-i\pi j_1} s^{j_1}_{\mathrm{ad}}\, |s^{j_2-j_1}_{\mathrm{bc}\bar{2}}|\, |s^{j_3-j_2}_{\bar{\mathrm{c}}2}| \\
& + \tau_1\tau_2\tau_3\,\mathrm{e}^{-i\pi(j_2-j_1)} |s^{j_1}_{\mathrm{a}\bar{\mathrm{c}}2}|\, |s^{j_2-j_1}_{\mathrm{bcd}}|\, |s^{j_3-j_2}_{\bar{\mathrm{c}}2}|\Big]. \qquad (4.2)
\end{aligned}$$

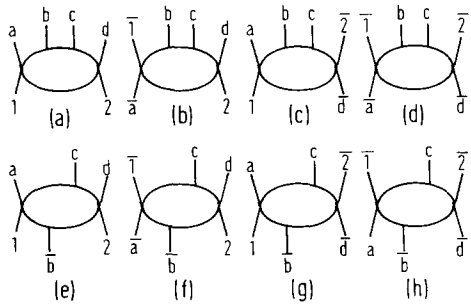

Fig. 8. The eight six-point amplitudes which are connected by crossing and analytic continuation.

The fully signatured amplitude then is interpreted as the sum of the right-hand cut contributions of the eight amplitudes of fig. 8*. For the last two terms in figs. 7a, b the situation is more complex. When following the simple recipe of adding up energy and phase factors of all eight amplitudes one neither arrives at the signature factors of the last two terms of the $2\to4$ amplitude nor at those of the $3\to3$ amplitude. This is because the last two terms of both the $2\to4$ and the $3\to3$ amplitudes in table 1 have, in fact, a *larger* discontinuity content than is suggested by the last two terms in figs. 7a, b. Since in the multi-Regge limit (4.1) several energy variables become indistinguishable from each other, we have the identities:

$$s^{j_3}s_{abc}^{j_1-j_3}s_{bc}^{j_2-j_1}\approx s^{j_1}s_{bcd}^{j_3-j_1}s_{bc}^{j_2-j_3}\approx s^{j_1+j_3-j_2}s_{ac}^{j_2-j_3}s_{bd}^{j_2-j_1}\approx s_{ac}^{j_1}s_{bd}^{j_3}s_{bc}^{j_2-j_1-j_3}, \tag{4.3}$$

$$\xi_{j_3}\xi_{j_1j_3}\xi_{j_2j_1}+\xi_{j_1}\xi_{j_3j_1}\xi_{j_2j_3}=\xi_{j_2j_3}\xi_{j_2j_1}\xi_{j_1+j_3-j_2}+\xi_{j_1}\xi_{j_3}\xi_{j_2-j_1-j_3}. \tag{4.4}$$

Hence it is not possible to distinguish between the analytic structure of the last two terms of fig. 7a and those of fig. 7c (which are the analytic continuations of the last two terms of fig. 7b): the last two terms of $T_{2\to4}$ in table 1 not only stand for the last two terms of fig. 7a but also for fig. 7c. In other words, contributions which have the analytic structure of fig. 7c can still be written *as if* they had the structure of the last two terms of fig. 7a, and the representation of table 1 does not require extra terms. Similarly, the last two terms of $T_{3\to3}$ in table 1 may contain contributions which do not correspond to the last two terms of fig. 7b but rather to those of fig. 7a (with suitable analytic continuation). For practical purposes this implies that if one computes, for example from multiple discontinuities, the five right-hand cut

* This interpretation, however, must not be oversimplified: there are non-planar unitarity contributions to $T_{2\to4}$ which cannot be reduced to a planar contribution to one of the eight amplitudes in fig. 8. They will be included if we note that the energy factors in (4.2) are not unique: for example, $s^{j_1}s_{bcd}^{j_2-j_1}s_{cd}^{j_3-j_2}$ also includes $s^{j_1}s_{bd}^{j_2-j_1}s_{cd}^{j_3-j_2}$.

contributions of figs. 7a, b for the $2\to4$ and $3\to3$ amplitudes, respectively, one may find some contributions for the $2\to4$ amplitude which are not simply analytic continuations of those which come from the $3\to3$ case. For the signatured amplitude one then has to *add* these distinct contributions such that the resulting amplitude has the right signature properties.

Within our calculational scheme we use the unitarity equation (2.1) as the definition of $T^{(2)}$ and do not attempt to compute multiple discontinuities. The r.h.s. of (2.1) determines single discontinuities, and we have to find the amplitude whose discontinuities agree with them. This requires us to be able to compute single discontinuities from the representations of table 1. For the first three terms this is rather straightforward: from (4.2) we know that there are discontinuities not only in $s = s_{abcd}$ but also in the variables s_{acd}, s_{abd}, and s_{ac} which are indistinguishable from s. For the sum of all these discontinuities we therefore find:

$$(\Delta_{abcd} + \Delta_{ad} + \Delta_{acd} + \Delta_{abd})\xi_{j_1}\xi_{j_2j_1}\xi_{j_3j_2}s^{j_1}s_{bcd}^{j_2-j_1}s_{cd}^{j_3-j_2} = -\xi_{j_2j_1}\xi_{j_3j_2}s^{j_1}s_{bcd}^{j_2-j_1}s_{cd}^{j_3-j_2}. \tag{4.5}$$

For the last two terms of the amplitudes $T_{2\to4}$ and $T_{3\to3}$ it will, in general, not be possible to determine individual single discontinuities but only sums of them: those contributions which correspond to the last two terms of fig. 7a will, for example, contribute to the discontinuity in s_{abc} but not s_{ac}, whereas those of the type fig. 7c contain an s_{ac} discontinuity but not an s_{abc} discontinuity. But since the r.h.s. of eq. (2.1) always gives the *sum* of both discontinuities, we do not run into counting problems. A similar argument argument holds for the $3\to3$ amplitude.

After these general remarks we now illustrate how the knowledge of analyticity properties will enable us to find from eq. (2.1) the $2\to4$ and $3\to3$ amplitudes of the matrix $T^{(2)}$. From this we then will extract the general $n\to m$ amplitude. Out of the $2^3 = 8$ signature configurations we only need to consider the cases $(\tau_1, \tau_2, \tau_3) = (+,+,+)$, $(+,-,-)$, $(-,+,-)$, $(-,+,+)$ and $(+,-,-)$ [the case $(-,-,-)$ belongs to $T^{(1)}$, and the remaining combinations follow from symmetry arguments]. We start with the case $(+,+,+)$. The requirement of having even signature in the t_1- and the t_3-channels restricts the quantum numbers in these channels to $I = 0$ or 2, but there is no restriction for the central t_2-channel. The r.h.s. of eq. (2.1) only determines the following discontinuities:

$$\Delta_{abcd}T^{(2)}_{2\to4}(+,+,+) = 2\pi\cdot\text{fig. 9a}\cdot\text{group weight}, \tag{4.6}$$

$$\Delta_{ad}T^{(2)}_{2\to4}(+,+,+) = 2\pi\cdot\text{fig. 9b}\cdot\text{group weight}, \tag{4.7}$$

$$\Delta_{abd}T^{(2)}_{2\to4}(+,+,+) = 2\pi\cdot\text{fig. 9c}\cdot\text{group weight}, \tag{4.8}$$

$$\Delta_{acd}T^{(2)}_{2\to4}(+,+,+) = 2\pi\cdot\text{fig. 9d}\cdot\text{group weight}. \tag{4.9}$$

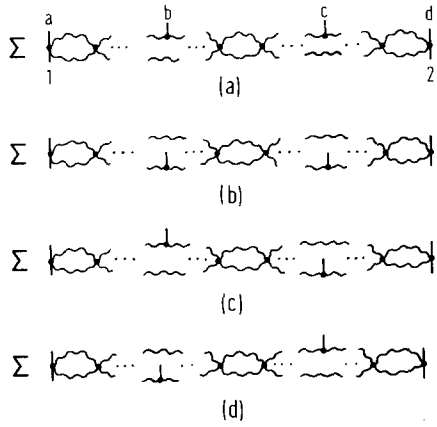

Fig. 9. Construction of $T^{(2)}_{2\to4}$ with signature (+, +, +): (a) the s discontinuity; (b) the s_{ac} discontinuity; (c) the s_{abd} discontinuity; (d) the s_{acd} discontinuity.

On the other hand, the use of table I and our previous discussion tell us that the amplitude is proportional to the sum of these discontinuities (we only keep leading terms in g^2 of the signature factors):

$$T^{(2)}_{2\to4}(+,+,+) = \frac{-is}{(2\pi i)^3}\left(\frac{2}{\pi}\right)^2 \int \mathrm{d}\omega_1\,\mathrm{d}\omega_2\,\mathrm{d}\omega_3 s_{ab}^{\omega_1} s_{bc}^{\omega_2} s_{cd}^{\omega_3}$$

$$\times\left[\frac{F_{LL}}{(\omega_2-\omega_1)(\omega_3-\omega_2)} + \frac{F_{RL}}{(\omega_1-\omega_2)(\omega_3-\omega_2)}\right.$$

$$+\frac{F_{RR}}{(\omega_2-\omega_3)(\omega_1-\omega_2)} + \frac{F^{(1)}_{LR}}{(\omega_1-\omega_3)(\omega_2-\omega_1)}$$

$$\left.+\frac{F^{(2)}_{LR}}{(\omega_3-\omega_1)(\omega_2-\omega_3)}\right], \tag{4.10}$$

$$(\Delta_{abcd}+\Delta_{acd}+\Delta_{abd}+\Delta_{ad})T^{(2)}_{2\to4}(+,+,+) = -iT^{(2)}_{2\to4}(+,+,+). \tag{4.11}$$

From this we find that:

$$T^{(2)}_{2\to4}(+,+,+) = \frac{2\pi is}{(2\pi i)^3}\int \mathrm{d}\omega_1\,\mathrm{d}\omega_2\,\mathrm{d}\omega_3 s_{ab}^{\omega_1} s_{bc}^{\omega_2} s_{cd}^{\omega_3}$$

$$\cdot[\text{figs. 9a + b + c + d}]\cdot\text{group weight}. \tag{4.12}$$

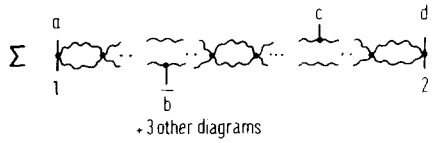

Fig. 10. Reggeon diagrams for $T^{(2)}_{3\to 3}$ with signature (+, +, +).

By similar arguments we obtain for $T^{(2)}_{3\to 3}$:

$$T^{(2)}_{3\to 3}(+,+,+) = \frac{2\pi i s}{(2\pi i)^3}\int \mathrm{d}\omega_1\,\mathrm{d}\omega_2\,\mathrm{d}\omega_3 s_{1b}^{\omega_1} s_{bc}^{\omega_2} s_{cd}^{\omega_3}\cdot[\text{figs. 10}]\cdot\text{group weight}. \tag{4.13}$$

As to the remaining energy discontinuities of $T^{(2)}_{2\to 4}$, the situation is similar to $T^{(2)}_{2\to 3}$ with signature (+, +). Eq. (2.1) gives no information about them, which means that they are of higher order in g^2 and will come in at a later stage of our calculations. We again expect the existence of equations of the type (3.13) which imply the self-consistency of our results: determining *combinations* of partial wave functions from *single* energy discontinuities must lead to the same answer as computing first, from *multiple* discontinuities, each partial wave *individually* and then forming their combinations. Although eq. (2.1) does not contain enough information for determining all partial wave functions separately but only combinations of them, this was, nevertheless, sufficient to determine the amplitude uniquely. This turns out to be true also for the other signature combinations which we have to compute: we always have just enough information to fix the amplitude to leading order in g^2.

In the case of the signature combination (+, −, −) the product $T^{(1)}T^{(1)+}$ determines, for the $2\to 4$ amplitude, the discontinuities in $s, s_{ad}, s_{acd}, s_{abd}$, in s_{abc}, s_{ac}, in s_{ab}, and the double discontinuity in s_{ab} and s_{cd}. They are shown in figs. 11a–d. They all have to be multiplied by the group weight diagram of fig. 11e: the t_1-channel has either $I = 0$ or 2 exchange, and the t_3-channel only allows for $I = 1$. For the production vertex we refer to $T^{(2)}_{2\to 3}(+,+)$ of sect. 3 and the appendix. Because of the signature structure, the amplitude is symmetric under twisting the t_1-channel, but antisymmetric in the t_3-channel. This implies that the discontinuities in s and s_{ad} are identical up to a minus sign, and similarly the s_{acd} and s_{abd} discontinuities. Therefore,

$$[\Delta_{abcd} + \Delta_{acd} + \Delta_{abd} + \Delta_{ad}]\,T^{(2)}_{2\to 4}(+,-,-) = 0. \tag{4.14}$$

From the same argument it also follows that

$$[\Delta_{abc} + \Delta_{ac}]\,T^{(2)}_{2\to 4}(+,-,-) = 0. \tag{4.15}$$

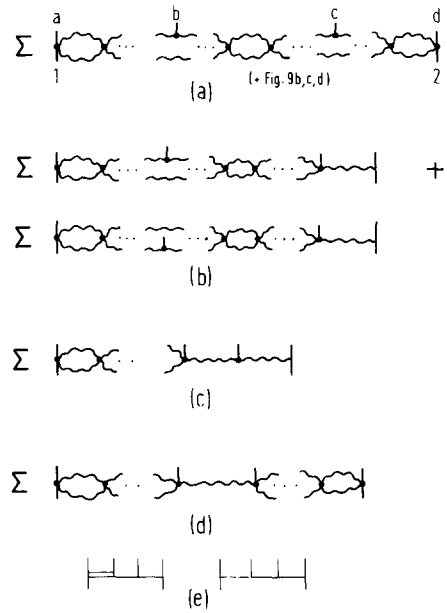

Fig. 11. Construction of $T^{(2)}_{2\to4}$ with signature $(+,-,-)$: (a) sum of the discontinuities in s, s_{ad}, s_{acd}, and s_{abd}; (b) sum of the discontinuities in s_{abc} and s_{ac}; (c) the s_{ab} discontinuity; (d) the double discontinuity in s_{ab} and s_{cd}; (e) a group weight diagram ($I = 2$ in the t_1-channel).

The double discontinuity in s_{ab} and s_{cd} can easily be shown to be of higher order in g^2 than a single discontinuity. Therefore, only the s_{ab} discontinuity remains and can be used for finding the $2\to4$ amplitude. From table 1, on the other hand, we find that to leading order in g^2 the amplitude is

$$T^{(2)}_{2\to4}(+,-,-) = \frac{s}{(2\pi i)^3}\int \mathrm{d}\omega_1\,\mathrm{d}\omega_2\,\mathrm{d}\omega_3 s^{\omega_1}_{ab} s^{\omega_2}_{bc} s^{\omega_3}_{cd} \times \left\{ \left(\frac{2}{\pi}\right)^2 (-i)\left[\frac{F_{RR}}{\omega_3(\omega_2-\omega_3)} + \frac{F_{RL}}{\omega_2(\omega_3-\omega_2)} \right] + \frac{2}{\pi}(-i)^2\left[\frac{F_{LL}}{\omega_3-\omega_2} + \frac{F^{(1)}_{LR}}{\omega_3} + \frac{F^{(2)}_{LR}}{\omega_2-\omega_3} \right] \right\}, \tag{4.16}$$

where we have expanded the signature factors and made use of the fact that the singularities in the ω_i are of the order g^2. Since all partial wave functions $F_{\dots}$ must be of the same order (they all are calculable from triple discontinuities), we conclude that in (4.16) only the first two terms should be kept. This implies that the

amplitude is proportional to its s_{ab} discontinuity:

$$\Delta_{ab}T^{(2)}_{2\to4}(+,-,-) = \frac{s}{(2\pi i)^3}\int d\omega_1\, d\omega_2\, d\omega_3 s_{ab}^{\omega_1} s_{bc}^{\omega_2} s_{cd}^{\omega_3} \times\left(\frac{2}{\pi}\right)^2(-)\left[\frac{F_{RR}}{\omega_3(\omega_2-\omega_3)}+\frac{F_{RL}}{\omega_2(\omega_3-\omega_2)}\right]. \quad (4.17)$$

For the other discontinuities we find, in agreement with (4.14) and (4.15), that they are down by one power of g^2 compared with the s_{ab} discontinuity, i.e., they are zero in our approximation. The final result for the $2\to4$ amplitude of this signature combination is

$$T^{(2)}_{2\to4}(+,-,-) = \frac{2\pi i s}{(2\pi i)^3}\int d\omega_1\, d\omega_2\, d\omega_3 s_{ab}^{\omega_1} s_{bc}^{\omega_2} s_{cd}^{\omega_3}\cdot\text{fig. 11c}\cdot\text{group weight}. \quad (4.18)$$

Repeating similar steps for the $3\to3$ amplitude of the same signature configuration we obtain

$$T^{(2)}_{3\to3}(+,-,-) = \frac{2\pi i s}{(2\pi i)^3}\int d\omega_1\, d\omega_2\, d\omega_3 s_{1\bar{b}}^{\omega_1} s_{\bar{b}c}^{\omega_2} s_{cd}^{\omega_3}\cdot\text{fig. 12}\cdot\text{group weight}. \quad (4.19)$$

The signature configurations $(+,+,-)$ and $(-,+,-)$ are treated in very much the same way. The crucial point is that several discontinuities on the r.h.s. of eq. (2.1) cancel among each other; from the amplitudes of table 1, on the other hand, one finds that these discontinuities are down by powers of g^2. As a result, the $2\to4$ amplitude for $(+,+,-)$ is proportional to its s_{abc} and s_{ac} discontinuities and the $(-,+,-)$ amplitude is proportional to its s_{bc} discontinuity. The results are

$$T^{(2)}_{2\to4}(+,+,-) = \frac{2\pi i s}{(2\pi i)^3}\int d\omega_1\, d\omega_2\, d\omega_3 s_{ab}^{\omega_1} s_{bc}^{\omega_2} s_{cd}^{\omega_3}\cdot\text{fig. 13}\cdot\text{group weight}, \quad (4.20)$$

$$T^{(2)}_{2\to4}(-,+,-) = \frac{2\pi i s}{(2\pi i)^3}\int d\omega_1\, d\omega_2\, d\omega_3 s_{ab}^{\omega_1} s_{bc}^{\omega_2} s_{cd}^{\omega_3}\cdot\text{fig. 14}\cdot\text{group weight}, \quad (4.21)$$

$$T^{(2)}_{3\to3}(+,+,-) = \frac{2\pi i s}{(2\pi i)^3}\int d\omega_1\, d\omega_2\, d\omega_3 s_{1\bar{b}}^{\omega_1} s_{\bar{b}c}^{\omega_2} s_{cd}^{\omega_3}\cdot\text{fig. 15}\cdot\text{group weight}, \quad (4.22)$$

$$T^{(2)}_{3\to3}(-,+,-) = \frac{2\pi i s}{(2\pi i)^3}\int d\omega_1\, d\omega_2\, d\omega_3 s_{1\bar{b}}^{\omega_1} s_{\bar{b}c}^{\omega_2} s_{cd}^{\omega_3}\cdot\text{fig. 16}\cdot\text{group weight} \quad (4.23)$$

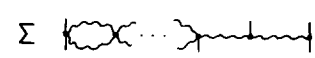

Fig. 12. The amplitude $T^{(2)}_{3\to3}$ with signature $(+,-,-)$.

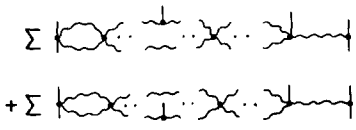

Fig. 13. The amplitude $T^{(2)}_{2\to 4}$ with signature (+, +, −).

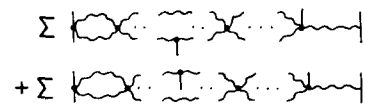

Fig. 15. The amplitude $T^{(2)}_{3\to 3}$ with signature (+, +, −).

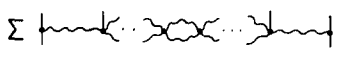

Fig. 14. The amplitude $T^{(2)}_{2\to 4}$ with signature (−, +, −).

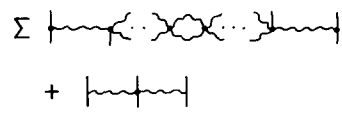

Fig. 16. The amplitude $T^{(2)}_{3\to 3}$ with signature (−, +, −).

(note the special contribution to $T^{(2)}_{3\to 3}$ coming from fig. 16: it gives rise to a new production vertex). In all these cases the r.h.s. of eq. (2.1) gives just enough information to determine, to leading order in g^2, the full amplitudes but not all partial wave functions separately.

Finally we note that the signature configuration (+, −, +) belongs to $T^{(3)}$ but not $T^{(2)}$. This follows from counting powers of g^2 [cf. the discussion after (3.19)]: all partial waves of $T^{(2)}_{2\to 4}$ are of the same order in g^2, namely $g^4 f(g^2/\omega)$. Because of the different signature factors, however, the amplitudes are not always of the same order: for (−, −, −) the amplitude is of the order $g^{-2} f(g^2/\omega)$, for (−, −, +), (+, +, +), (−, +, −) and (−, +, +) we have $g^0 f(g^2/\omega)$, but for (+, −, +) the amplitude goes like $g^2 f(g^2/\omega)$. This case therefore belongs to the following step within our scheme.

We now try to generalize to $T^{(2)}_{n\to m}$. For this we do not offer a general proof but rather rely upon the belief that the six-point amplitudes already contain all essential features of the analytic structure of multiparticle amplitudes. For general $T^{(2)}_{n\to m}$ we state the following rules:

(i) $T^{(2)}$ contains $n\to m$ amplitudes where the number of t-channels with even signature t_{even} is greater or equal to one (the case $t_{\text{even}} = 0$ belongs to $T^{(1)}$). If t_{even} is greater than one, the even signatured t-channels must be connected, i.e., there is no odd signature t-channel between two even signature t-channels. Otherwise the amplitude is down by one (or more) powers of g^2 and belongs to $T^{(n)}$ with $n \geqslant 3$.

(ii) The amplitude $T^{(2)}_{n\to m}$ can always be cast into the form

$$T^{(2)}_{n\to m} = \frac{2\pi i s}{(2\pi i)^p} \int \mathrm{d}\omega_1 \ldots \mathrm{d}\omega_p s^{\omega_1}_{\mathrm{ab}} \ldots s^{\omega_p}_{\mathrm{yz}} F_{n\to m}(\omega_i, t_i, \eta_{ij}) . \tag{4.24}$$

The Mellin transform $F_{n\to m}$ which is a combination of the various partial wave functions and signature factors, can be described in a diagrammatic way [cf. the

Fig. 17. The elements of the reggeon calculus for $T^{(2)}$.

discussion after (2.10)]. The elements of this reggeon calculus are shown in fig. 17. $F_{n\to m}$ then consists of all possible diagrams with the restriction that any odd signature t-channel has only one reggeon intermediate states whereas an even signature t-channel has two reggeon intermediate states. (Note that the production vertex in fig. 17 stands for a "contracted" even signature t-channel). The quantum numbers are restricted only for the two t-channels which couple to the external particles ($I = 1$ for odd, $I = 0, 2$ for even signature, respectively) and for all t-channels with a single reggeon line ($I = 1$ always).

5. The zero-mass limit

The strongest motivation for investigating the high-energy behavior of non-abelian gauge theories comes from the question what the dynamics is in the vacuum exchange channel (the nature of the pomeron). Within our scheme of calculating a unitary high-energy description, $T^{(2)}$ is the lowest approximation in which this quantum number configuration appears ($I = 0$, even signature). The $2\to 2$ amplitude $T^{(2)}_{2\to 2}$ which can be represented in terms of an integral equation has been studied by two groups [2, 3] and it has been shown that the leading j-plane singularity in the vacuum channel is a fixed cut to the right of $j = 1$. This makes it clear that higher terms in our expansion (1.6) will be essential in order to restore the unitarity bounds which are violated by $T^{(2)}$. It will, therefore, be one of the most important parts of our program to find a method which allows us to sum all the terms of (1.6). An observation made by Lipatov et al. [10] could serve as a starting point for developing a summation technique: they noticed that the formation of the fixed cut vacuum singularity in $T^{(2)}_{2\to 2}$ is intimately related to a diffusion of the wee partons which, formally, requires infrared finiteness of the amplitude $T^{(2)}_{2\to 2}$ in the limit where the vector particle mass goes to zero. This diffusion dynamics can be generalized (as we shall discuss elsewhere [6]) to include higher-order terms in the expansion (1.6), provided that the limit $M\to 0$ can be shown to exist also for the higher $T^{(n)}$. We therefore perform a somewhat systematic study of this limit*. In this section, we show that, order by order in perturbation theory, $T^{(2)}_{2\to 2}$ is finite and well-behaved when $M\to 0$. This proof will then be generalized to parts of higher $T^{(n)}$: this will help us in studying the effect of higher $T^{(n)}$ in the pomeron channel.

* That the zero-mass limit exists in lowest non-trivial order perturbation theory was communicated to me by L.N. Lipatov. This result has also been stated in ref. [11].

Another reason for being interesting in the zero-mass limit comes from the hope that our calculations can also be used for the Regge limit of pure Yang-Mills theories (QCD). As we have explained elsewhere [5], the Regge limit lies, in a certain sense, not far from the hard scattering region where perturbation theory can safely be applied, and the introduction (via the Higgs mechanism) of a mass for the vector particles (gluons) then serves as a convenient way of avoiding infrared problems within perturbation theory. The question whether, at least in the Regge limit, the zero-mass limit of the Higgs model agrees with the high-energy limit of QCD is still unresolved, but recent calculations [12] indicate that this may be the case (at least at the level of $T^{(2)}$). At the present state we shall only show that the limit $M \to 0$ exists and is well-defined (in a sense which will be specified later): after summing all terms in (1.6) it then will have to be shown to what extent the final result is dependent on M at all.

As a result of our unitarization scheme, the elements of $T^{(2)}$ come in form of a reggeon calculus. For the case of the $2 \to 2$ amplitude, the diagrams are shown in fig. 2. In order to have an analytic expression we define a (non-amputated) reggeon particle scattering amplitude $\varphi(k, q-k; \omega)$ which is given by the following integral equation:

$$\begin{aligned}
&\big[\omega + 2 - \alpha(k) - \alpha(q-k)\big]\varphi(k_\perp, q_\perp - k_\perp; \omega) \\
&\quad = g^2\omega\big[-2H_{vv}^2 - H_{sv}^2\big] + \frac{-2g^2}{(2\pi)^3}\int \mathrm{d}^2k'_\perp\, K(k_\perp, q_\perp - k_\perp; k'_\perp, q_\perp - k'_\perp) \\
&\qquad \times \frac{1}{k'^2_\perp + M^2}\,\frac{1}{(q-k')^2_\perp + M^2}\varphi(k'_\perp, q_\perp - k'_\perp; \omega)\,. \qquad (5.1)
\end{aligned}$$

In the vacuum channel the kernel $K(k, q-k; k', q-k')$ has the form

$$\begin{aligned}
K(k_\perp, q_\perp - k_\perp; k'_\perp, q_\perp - k'_\perp) &= \big(-q_\perp^2 - \tfrac{5}{2}M^2\big) \\
&+ \frac{(k'^2_\perp + M^2)\big((q-k)^2_\perp + M^2\big) + (k^2_\perp + M^2)\big((q-k')^2_\perp + M^2\big)}{(k-k')^2_\perp + M^2}\,. \qquad (5.2)
\end{aligned}$$

The connection between φ and the Mellin transform of $T^{(2)}_{2\to 2}$, $F_{2\to 2}$, is

$$\omega F_{2\to 2}(q^2) = \int \frac{\mathrm{d}^2k'_\perp}{(2\pi)^3}\,\frac{\varphi(k'_\perp, q_\perp - k'_\perp; \omega)}{(q-k')^2_\perp + M^2}\,\frac{1}{k'^2_\perp + M^2}\,g^2\big[-2H_{vv}^2 - H_{sv}^2\big]\,. \qquad (5.3)$$

Since the trajectory function $\alpha(t)$ [eqs. (4.6) and (4.9) of I] is singular when M goes to zero, this way of representing φ is not very convenient. Following ref. [10] we rather rewrite the integral equation (5.1) in such a way, that the new kernel is directly proportional to g^2/ω:

$$\varphi(k_\perp, q_\perp - k_\perp; \omega) = g^2\left[-2H_{vv}^2 - H_{vs}^2\right]$$

$$+\frac{-2g^2}{(2\pi)^3\omega}\int d^2k'_\perp K(k_\perp, q_\perp - k_\perp; k'_\perp, q_\perp - k'_\perp)$$

$$\times \frac{1}{k'^2_\perp + M^2}\frac{1}{(q-k')^2_\perp + M^2}\varphi(k'_\perp, q_\perp - k'_\perp; \omega)$$

$$+\frac{\alpha(k)+\alpha(q-k)-2}{\omega}\varphi(k_\perp, q_\perp - k_\perp; \omega) \qquad (5.4)$$

(the Neumann expansion of this equation coincides with the power series expansion of φ in g^2/ω). Before taking the limit $M \to 0$, it is necessary to change the inhomogeneous term which represents the coupling of the exchanged vector particles to the external particles: as it is well known (e.g., from calculations with QED [13]), the simplest example for a high-energy scattering amplitude which is finite when the exchanged vector particles have zero mass is photon-photon scattering (fig. 18). The photon dissociates into a fermion-antifermion pair (which for simplicity is taken to be massive), and the fermions then interact by exchanging vector particles. The infrared finiteness of this amplitude is due the fact that the fermion loop produces a zero when the momentum of one of the two attached photons goes to zero. Replacing the external photons by vector mesons and taking for the vertex meson-fermion-antifermion a hadronic wave function (e.g., $\rho \to q\bar{q}$), one obtains a simple model in which the massless gluons can couple to a $q\bar{q}$-bound state. In the following we shall use this function $\varphi_0(k, q-k)$ as the inhomogeneous term in the integral equations (5.1) or (5.4). We do not need to present the analytic expression of φ_0: the only property which is relevant for our purposes is its vanishing as a

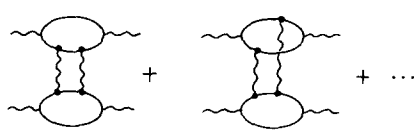

Fig. 18. Simplest model for a infrared finite $2 \to 2$ scattering amplitude: photon-photon scattering in QED. The sum goes over all possibilities of attaching the two exchanged photons to the fermion loops.

function of one of its arguments:

$$\varphi_0(k_\perp, q_\perp - k_\perp) = |k_\perp| \cdot \text{const}, \qquad \text{if } |k_\perp| \to 0,$$

$$= |q_\perp - k_\perp| \cdot \text{const}, \qquad \text{if } |q_\perp - k_\perp| \to 0. \tag{5.5}$$

We shall now show that, order by order in perturbation theory, the solution φ to the integral equation (5.4) (with the inhomogeneous term replaced by φ_0) is well-behaved and finite when the mass of the vector particle M^2 is taken to zero. Moreover, the property (5.5) of the inhomogeneous term is preserved, i.e., the solution φ has this property at each order of g^2 (up to powers of $\ln|k|$ or $\ln|q-k|$). By iterating the integral equation, the solution is represented as a power series in g^2/ω:

$$\varphi(k_\perp, q_\perp - k_\perp; \omega) = \sum_{n=0}^{\infty} \left(\frac{g^2}{\omega}\right)^n \varphi_n(k_\perp, q_\perp - k_\perp). \tag{5.6}$$

For the coefficient functions we have the recursion relation:

$$\varphi_{n+1}(k_\perp, q_\perp - k_\perp) = \frac{-2}{(2\pi)^3} \int \mathrm{d}^2 k'_\perp K(k_\perp, q_\perp - k_\perp; k'_\perp, q_\perp - k'_\perp)$$

$$\times \frac{1}{k'^2_\perp + M^2} \frac{1}{(q-k')^2_\perp + M^2} \varphi_n(k'_\perp, q_\perp - k'_\perp)$$

$$+ \frac{\alpha(k) + \alpha(q-k) - 2}{g^2} \varphi_n(k_\perp, q_\perp - k_\perp). \tag{5.7}$$

The first term in (5.6), φ_0, is independent of M^2 and satisfies (5.5). We now assume that φ_n has already been shown to have the desired properties and demonstrate that the recursion relation for φ_{n+1} does not destroy them. In the limit $M \to 0$, the integral in (5.7) can be simplified (for convenience, we slightly change the notation of the variables and write the expressions for $\alpha(k)$ in a somewhat special way [10]):

$$\varphi_{n+1}(q_1, q_2) = \frac{2}{(2\pi)^3} \Bigg\{ \int \mathrm{d}^2 k'_\perp \frac{1}{(q_1 + k')^2_\perp (q_2 - k')^2_\perp} 2 \left(\boldsymbol{q}_1 + \boldsymbol{k}' \frac{q_{1\perp}^2}{k'^2_\perp} \right)_\perp$$

$$\cdot \left(\boldsymbol{q}_2 - \boldsymbol{k}' \frac{q_{2\perp}^2}{k'^2_\perp} \right)_\perp \varphi_n(q_1 + k'_\perp, q_2 - k'_\perp \omega)$$

$$+ \int \frac{\mathrm{d}^2 k'_\perp}{k'^2_\perp} \left(\frac{q_{1\perp}^2}{k'^2_\perp + (q_1 + k')^2_\perp} + \frac{q_{2\perp}^2}{k'^2_\perp + (q_2 - k')^2_\perp} \right)$$

$$\times \varphi_n(q_1, q_2) + O(M^2) \Bigg\}. \tag{5.8}$$

As long as $q_1 \neq q_2$ and $q_1 \neq 0$, $q_2 \neq 0$ this integral is well-behaved and finite: the pole at $k'_\perp = -q_{1\perp}$ is cancelled by a zero in $\boldsymbol{q}_{1\perp} + \boldsymbol{k}'_\perp q_{1\perp}^2/k'^2_\perp$, and near $k'_\perp = 0$ there is a cancellation between the two integrals. For $q_{1\perp} \to -q_{2\perp} \neq 0$ the first integral tends to diverge logarithmically near $k'_\perp = q_{2\perp}$, but the property (5.5) of φ_n produces a zero in the numerator which kills the divergence. Now we take $q_{1\perp} \to 0$ with $q_{2\perp} \neq 0$. For all values of $k'_\perp$ away from zero, say $|k'_\perp| > \varepsilon$, each part of the integral (5.8) is finite by itself and vanishes as $|q_{1\perp}|$. The integration part with $|k'_\perp| < \varepsilon$ can be estimated by using (5.5):

$$\varphi_n(q_{1\perp} + k'_\perp, q_{2\perp} - k'_\perp) = (\boldsymbol{q}_{1\perp} + \boldsymbol{k}'_\perp)\cdot[\boldsymbol{a} + \boldsymbol{b}\,O(|k'|)]$$

$$\varphi_n(q_{1\perp}, q_{2\perp}) = \boldsymbol{q}_{1\perp}\cdot\boldsymbol{a} \tag{5.9}$$

(neglecting powers of logarithms which are not essential for the argument). We find that this part of the integral behaves like:

$$\varphi_{n+1}(q_1, q_2) = |q_{1\perp}|\cdot(\ln q_{1\perp}^2)^p\cdot\text{const} \tag{5.10}$$

(the power of the logarithms has increased by one, compared with φ_n). Finally, for $|q_{1\perp}| \sim |q_{2\perp}| \sim \lambda \to 0$, the part of the integral with $|k'_\perp| > \varepsilon$ goes like $\boldsymbol{q}_{1\perp}\cdot\boldsymbol{q}_{2\perp} \sim \lambda^2$. The region $|k'_\perp| < \varepsilon$ behaves as $\lambda^2(\ln\lambda)^p$, where again the power of logarithms has increased by one compared with φ_n. This then completes our assertion that each $\varphi_n(k, q-k)$ has, up to powers of logarithms, the same properties (infrared finiteness and (5.5)) as the inhomogeneous term φ_0. The fact that each φ_n has the property (5.5), ensures that the integral (5.3) (with the vertex $[g^2 H_{vv}]$ being replaced by another φ_0) does not blow up when $M^2 \to 0$.

We now show how this result can be used in order to prove the infrared finiteness of higher-order terms $T^{(n)}$ in the expansion (1.6). What we have constructed so far, are only the first two terms: $T^{(1)}$ in paper I and $T^{(2)}$ in this paper. The construction of the higher $T^{(n)}$ will be described in future publications, in particular the form of the general (the reggeon number non-conserving) $n \to m$ reggeon interaction vertex. It is, however, already clear at the present stage of our calculations that some contributions to $T_{2\to 2}^{(n)}$ ($n \geqslant 2$) will be of the form shown in fig. 19: this are those reggeon diagrams in which the number of reggeons in the t-channel is conserved. They alone are not sufficient for satisfying s-channel unitarity in all subenergy variables*, and what is missing are those diagrams in which the reggeon number changes. In view of the task of finding a summation technique for all reggeon diagrams it is, however, reasonable to start with those of

* In a series of papers, Cheng et al. [12] have claimed that the unitary S-matrix takes the form of an eikonal operator: by expanding this eikonal expression one obtains exactly the diagrams of fig. 19. As explained above, these diagrams are not sufficient to satisfy unitarity: the eikonal result therefore represents only a part of the complete high-energy description.

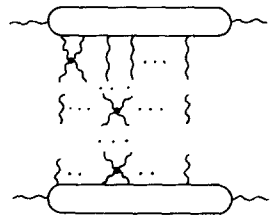

Fig. 19. Reggeon diagrams of $T^{(n)}_{2\to 2}$ for which the zero-mass limit can be shown to exist: the quartic vertex is the same as in fig. 17, and for the coupling to the external particles we assume the property (5.11).

fig. 19, because they represent, in a certain sense, the most simple ones. In this paper we therefore demonstrate that these diagrams are, in the pomeron channel, finite when M^2 is taken to zero; use of this result will be made in a separate paper.

The argument is very similar to that of $T^{(2)}_{2\to 2}$. We first define a two particle-n reggeon function $\varphi\ (k_1,\ldots,k_n)$ (the momenta k_i are restricted such that $\Sigma_{i=1}^n k_i = q$) which represents the sum of all diagrams of fig. 19 except the lower vertex. For the coupling of the reggeized vector particles to the external particles we take a vertex function $\varphi_0\ (k_1,\ldots,k_n)$ which does not depend on the vector mass M^2 and satisfies the condition (5.5):

$$\varphi_0(k_{1\perp},\ldots,k_{n\perp}) \sim |k_{i\perp}| \cdot \text{const}, \qquad i = 1,\ldots,n \tag{5.11}$$

(we expect that the simplest model for this function is, again, a quark loop with the vector particles being attached in all possible ways). Before we write the integral equation for $\varphi\ (k_1,\ldots,k_n)$ we have to analyze the group structure. For the interaction of two reggeon lines i and j the coupling function is (in the limit $M^2 \to 0$):

$$K(k_{i\perp},k_{j\perp};k_{i\perp}+k_\perp,k_{j\perp}-k_\perp) = \left(\boldsymbol{k}_i + \boldsymbol{k}\frac{k_{i\perp}^2}{k_\perp^2}\right)_\perp \cdot \left(\boldsymbol{k}_j - \boldsymbol{k}\frac{k_{j\perp}^2}{k_\perp^2}\right)_\perp , \tag{5.12}$$

with the group weight factor (cf. (4.6) of I):

$$\varepsilon_{a_i r b_i}\varepsilon_{a_j b_j r} = -2P_0(a_i a_j|b_i b_j) - P_1(a_i a_j|b_i b_j) + P_2(a_i a_j|b_i b_j)\,. \tag{5.13}$$

The tensor (5.13) indicates that the two lines can be in a state with $I = 0$, 1, or 2. Since the total quantum number of all reggeon lines is restricted to $I = 0$, we define the projection operator onto the $I = 0$ state*:

$$P_0 = \text{const} \cdot \prod_{k=1}^{n} \left(\sum_{i<j} \boldsymbol{t}_i \cdot \boldsymbol{t}_j + n - \tfrac{1}{2}k(k+1) \right) \tag{5.14}$$

* For the construction of the projection operator we have used ref. [13].

where $(t_i^a)_{mn} = -i\varepsilon_{amn}$ is the isospin matrix for the line i and the normalization is such that $P_0^2 = P_0$. From the condition

$$0 = \text{const} \cdot \prod_{k=0}^{n} \left(\sum_{i<j} \boldsymbol{t}_i \cdot \boldsymbol{t}_j + n - \tfrac{1}{2}k(k+1) \right)$$

$$= P_0 \left(\sum_{i<j} \boldsymbol{t}_i \cdot \boldsymbol{t}_j + n \right), \tag{5.15}$$

it follows that

$$P_0 \sum_{i<j} \boldsymbol{t}_i \cdot \boldsymbol{t}_j = -nP_0, \tag{5.16}$$

and

$$P_0 \boldsymbol{t}_a \cdot \boldsymbol{t}_b = -\frac{2}{n-1} P_0. \tag{5.17}$$

Hence each kernel K_{ij} in (5.12) comes with the weight $-(2/(n-1))P_0$, and the integral equation for $\varphi(k_1, \ldots k_n)$ is

$$\left[\omega + n - \sum_{i=1}^{n} \alpha(k_i^2) \right] \varphi(k_{1\perp}, \ldots k_{n\perp}; \omega) = \omega \varphi_0(k_{1\perp}, \ldots k_{n\perp}; \omega)$$

$$+ \frac{g^2}{(2\pi)^3} \frac{-2}{n-1} \sum_{i<j} \int \mathrm{d}^2 k_\perp K(k_{i\perp}, k_{j\perp}, k_{i\perp} + k_\perp, k_{j\perp} - k_\perp)$$

$$\times \frac{1}{(k_i + k)_\perp^2 (k_j - k)_\perp^2} \varphi(k_{1\perp}, \ldots, k_{i\perp} + k_\perp, \ldots k_{j\perp} - k_\perp, \ldots k_{n\perp}; \omega). \tag{5.18}$$

It is convenient to rewrite this equation in such a way that the Neumann expansion coincides with the power-series expansion in g^2/ω:

$$\varphi(k_{1\perp}, \ldots, k_{n\perp}; \omega) = \varphi_0(k_{1\perp}, \ldots k_{n\perp}) + \frac{g^2}{(2\pi)^3} \frac{-2}{n-1} \sum_{i<j} \int \mathrm{d}^2 k_\perp$$

$$\times K(k_{i\perp}, k_{j\perp}; k_{i\perp} + k_\perp, k_{j\perp} - k_\perp) \frac{1}{(k_i + k)_\perp^2 (k_j - k)_\perp^2}$$

$$\times \varphi(k_{1\perp}, \ldots, k_{i\perp} + k_\perp, \ldots k_{j\perp} - k_\perp, \ldots k_{n\perp}; \omega)$$

$$+ \frac{1}{\omega} \frac{1}{n-1} \sum_{i<j} \left[\alpha(k_i) + \alpha(k_j) - 2 \right] \varphi(k_1, \ldots k_n; \omega). \tag{5.19}$$

We now see that the kernel of this integral equation is a sum of combinations $(-2K(k_i k_j; k_i + k, k_j - k) + \alpha(k_i) + \alpha(k_j) - 2)/(n-1)$: for this expression we have shown [cf. (5.8)] that when it acts on φ_n, which satisfies (5.5) and is infrared finite, it reproduces these properties also for φ_{n+1}. The kernel in (5.19) therefore has the same property, and our function φ will be infrared finite to any order in g^2/ω.

This completes our study of the zero-mass limit. What we have shown—first for $T^{(2)}_{2\to 2}$, then for parts of $T^{(n)}_{2\to 2}$ with $n \geqslant 2$ in the vacuum exchange channel—is that, with a suitable coupling of the exchanged vector particles to the external particles, the amplitudes are finite and well defined in the limit $M^2 \to 0$. For this argument it was essential that the various terms in the kernel of (5.8) and (5.19) come just with the right weight to cancel possible infrared divergences.

6. Summary and outlook

In this paper we have constructed the first non-leading term in expansion (1.6) for a completely unitary high-energy S-matrix of a spontaneously broken non-abelian gauge theory. Eq. (2.1) which defines this term $T^{(2)}$, determines the single energy discontinuities of the $n \to m$ amplitudes, and we have made full use of the analytic structure of multiparticle amplitudes in the Regge limit in order to reconstruct the amplitudes out of these single discontinuities. The resulting amplitudes $T^{(2)}_{n\to m}$ (our calculations went up to the six-point amplitudes and then generalized to the $n \to m$ case) come in form of a reggeon calculus with one (odd signature) or two (even signature) reggeons in each t-channel. The elements of this reggeon calculus are given in fig. 17, and their analytic form follows from the rules of the appendix.

For the most interesting case, the vacuum exchange channel (pomeron), we have studied the zero-mass limit. After replacing the external particles by an appropriate model for a $q\bar{q}$ bound state one finds that the amplitude $T^{(2)}_{2\to 2}$ is finite in the limit $M^2 \to 0$, order by order in perturbation theory, and we have extended this proof to larger classes of reggeon diagrams which are subsets of $T^{(n)}_{2\to 2}$ with $n > 2$. Use of these results will be made in a separate paper.

Together with ref. [1], this paper represents the first two parts of a program whose aim is the construction of a unitary high-energy description of massive Yang-Mill theories. Although the basic idea has not changed—to use the lagrangian of the theory only for the computation of tree elements and to find all other contributions from unitarity—the procedure of the present paper slightly differs from I. The elements of $T^{(1)}$ have been calculated order by order in perturbation theory; in the present paper we used the results of I (which are of infinite order) and eq. (2.1) in order to find the elements of $T^{(2)}$. In order to find the remaining terms $T^{(n)}$ with $n > 2$ in the expansion (1.6), we will, in essence, repeat these two steps. At the level of $T^{(3)}$, new subtraction constants appear (this can most easily be seen by expanding the three reggeon exchange amplitude in powers of g^2: the

lowest term is of the order $s \cdot g^6$ and real-valued), and it is, therefore, not sufficient to just iterate the unitarity equation. It is rather necessary to compute these new subtraction constants in the same way, as the tree approximations were found for $T^{(1)}$, and then to continue order by order in perturbation theory. At the level of $T^{(4)}$, one repeats the step which has been done in this paper. The results of these calculations will be a complete reggeon calculus with computable elements. The most interesting part of this is the form of the general $n \to m$ reggeon interaction vertex, for which, at least in the limit of small M^2, a simple form is expected to exist [in analogy to (5.12) for the $2 \to 2$ vertex].

Apart from the task of completing the derivation of the full reggeon calculus, we are also faced with the problem of being able to *sum all the terms in the expansion* (1.6), i.e., of understanding how the higher terms change the result of the first approximation $T^{(2)}$. As we have outlined elsewhere [5], two approaches are emerging: the first one tries to make use of the apparatus of reggeon field theory [14], the other one starts from the diffusion picture which has been found in ref. [10]. For both approaches it will be absolutely essential to know the form of the general $n \to m$ reggeon vertex, but attempts to formulate such schemes should be made already at the present stage.

During two visits to CERN I had very useful discussions with A.R. White about the analytic structure of multiparticle amplitudes. Both his support and the hospitality of the CERN Group are gratefully acknowledged.

Note added

After this paper was written a publication of Ya.Ya. Balitskij and L.N. Lipatov was brought to our attention (Yad. Fiz. 28 (1978) 1597) in which a similar proof is given for the infrared finiteness of $T^{(2)}_{2\to 2}$.

Appendix

In this appendix we briefly describe how the momentum (helicity) structure of reggeon particle vertices can be computed. All necessary calculations have been done in I (sect. 4 and the appendix), and we only have to make repeated use of them. For the calculation of production vertices typically the following situation emerges. When computing, say, the s_{bc} discontinuity of a $2 \to 3$ amplitude (cf. fig. 6c), we have to multiply the two-reggeon particle vertex with the two particle reggeon vertex, the former being a 3-component vector in helicity space and the latter one a 3×3 matrix. The production vertex is most easily expressed in the center of mass system (c.m.s.) of the $2 \to 3$ amplitude, whereas the $2 \to 2$ scattering in the (bc) system is most conveniently expressed in the c.m.s. of the bc channel. It is, therefore, necessary to perform a Lorentz transformation from one coordinate system to the other, and it is the kinematics of this transformation that we need for the calculation of production vertices. In the following we will calculate the central vertex of fig. 20, going step by step from the left- to the right-hand side.

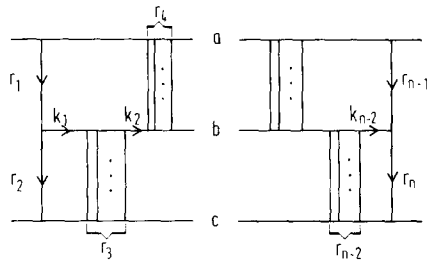

Fig. 20. Construction of a general reggeon self-interaction vertex.

The left-most element is the production vertex $\Gamma(r_1, -r_2)$ [cf. eqs. (3.6) and (3.7) of I] in the overall c.m.s. It is given by the 3-component vector:

$$\Gamma^{\mathrm{T}} = \left(\Gamma_\sigma e^1_\sigma, \Gamma_\sigma e^2_\sigma, \Gamma_\sigma e^3_\sigma\right) \tag{A.1}$$

(the polarization vectors e^1 and e^2 refer to the transverse polarization, the vector e^3 to the longitudinal one). In order to compute the unitarity integral in the (bc) system, we transform to the c.m.s. of the particles b and c. The transformation matrix is $L_{\mathrm{bc}}(k_1)$:

$$L_{\mathrm{bc}}(k_1) = \begin{bmatrix} A_{\mathrm{bc}} & 0 & -B_{\mathrm{bc}} \\ 0 & 1 & 0 \\ B_{\mathrm{bc}} & & A_{\mathrm{bc}} \end{bmatrix} \tag{A.2}$$

$$A_{\mathrm{bc}} = \frac{\sqrt{s}}{|k_1| s_{\mathrm{bc}}}\left(-M^2 + \frac{s_{\mathrm{bc}}}{s}(s_{\mathrm{ab}} + s_{\mathrm{bc}})\right), \tag{A.3}$$

$$B_{\mathrm{bc}} = \frac{|k_{1\perp}| M\sqrt{s}}{|k_1| s_{\mathrm{bc}}}\,. \tag{A.4}$$

When multiplying the vector Γ in (A.1) by this matrix L_{bc}, we obtain [cf. (4.29) of I]:

$$\Gamma^{\mathrm{T}} L_{\mathrm{bc}} = (-i)\left[V(r_{1\perp}, k_{1\perp}) - Me_3 - \frac{r_1^2 - M^2}{-k_{1\perp}^2 - M^2}\left(V(k_{1\perp}, k_{1\perp}) - 2Me_3\right)\right]^{\mathrm{T}}, \tag{A.5}$$

$$V(r_{1\perp}, k_{1\perp}) = \begin{bmatrix} 2|r_{1\perp}| \cos(r_{1\perp}, k_{1\perp}) \\ 2|r_{1\perp}| \sin(r_{1\perp}, k_{1\perp}) \\ 0 \end{bmatrix}, \qquad e_3 = \begin{bmatrix} 0 \\ 0 \\ 1 \end{bmatrix}. \tag{A.6}$$

For the subsequent scattering process in the (bc) channel which consists of the exchange of N_3 vector particles we have, for the upper vertex, the matrix $R(k_{1\perp}, k_{2\perp})(H_{vv})^{N_3}$, where $k_{1\perp}$ and $k_{2\perp}$ are the initial and final transverse momenta:

$$R(k_{1\perp}, k_{2\perp}) = \begin{pmatrix} \cos\theta & \sin\theta & 0 \\ -\sin\theta & \cos\theta & 0 \\ 0 & 0 & 1 \end{pmatrix},$$

$$\theta = \text{angle between } k_{1\perp} \text{ and } k_{2\perp}. \tag{A.7}$$

Multiplication with (A.5) leads to:

$$\Gamma^{T} L_{bc} R H_{vv}^{N_3} = (-i)(-1)^{N_3} \Big[V(r_{1\perp}, k_{2\perp}) - \left(\tfrac{1}{2}\right)^{N_3} M e_3 - \frac{r_1^2 - M^2}{-k_{1\perp}^2 - M^2} \left(V(k_{1\perp}, k_{2\perp}) - \left(\tfrac{1}{2}\right)^{N_3 - 1} M e_3 \right) \Big]^{T}. \tag{A.8}$$

In order to return to the c.m.s. of the particles a, b, and c, we multiply with $L_{bc}^{T}(k_2)$:

$$\Gamma^{T} L_{bc} R H_{vv}^{N_3} L_{bc}^{T} = (-1)^{N_3} \Big[\Gamma(r_1, -r_{23}) + \left(1 - \frac{1}{2^{N_3}}\right)(-i) M L_{bc} e_3 - \frac{r_1^2 - M^2}{-k_{1\perp}^2 - M^2} \times \left(\Gamma(k_{1\perp}, -r_3) + \left(1 - \frac{1}{2^{N_3 - 1}}\right)(-i) M L_{bc} e_3 \right) \Big]^{T}. \tag{A.9}$$

The two terms of (A.9) are illustrated in fig. 21. This result only includes the production of vector particles. If the produced particle with momentum k_1 is a Higgs scalar, the result is, instead of (A.9), simply const. $\times (M e_3)^{T}$; the contribution of a Higgs scalar somewhere between k_1 and k_2 leads to (A.9), but without the terms $\Gamma(r_1, -r_{23})$ and $\Gamma(k_1, -r_3)$.

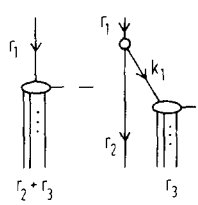

Fig. 21. Momentum structure of the production vertex (A.9).

Next we compute a unitarity integral in the (ab) system. The transformation which takes us from the (abc) c.m.s. to the (ab) c.m.s. is $L_{ab}(k_2)$. It has the same form as (A.2), and the elements are

$$A_{ab} = \frac{\sqrt{s}}{|k_2| s_{ab}} \left(-M^2 + \frac{s_{ab}}{s} (s_{ab} + s_{bc}) \right), \tag{A.10}$$

$$B_{ab} = \frac{-|k_{2\perp}| M \sqrt{s}}{|k_2| s_{ab}} . \tag{A.11}$$

$$L^T_{ab}(k_2) L_{bc}(k_1) e_3 = e_3 - \frac{M}{-k^2_{2\perp} - M^2} (V(k_{2\perp}, k_{2\perp}) + 2Me_3), \tag{A.12}$$

and

$$\Gamma(r_1, -r_{23}) L_{ab}(k_2) = (-i) \Bigg[V(-r_{23\perp}, k_{2\perp}) + Me_3 - \frac{r^2_{23} - M^2}{-k^2_{2\perp} - M^2} (V(k_{2\perp}, k_{2\perp}) + 2Me_3) \Bigg]^T . \tag{A.13}$$

Multiplication of (A.9) with L_{ab} therefore leads to:

$$\begin{aligned} &\Gamma^T L_{bc} R H^{N_3}_{vv} L^T_{bc} L_{ab} \\ &= (-1)^{N_3} (-i) \Bigg\{ V(-r_{23\perp}, k_{2\perp}) + \left(2 - \frac{1}{2^{N_3}}\right) Me_3 - \frac{r^2_{23} - \left(2 - \frac{1}{2^{N_3}}\right) M^2}{-k^2_{2\perp} - M^2} \\ &\quad \times (V(k_{2\perp}, k_{2\perp}) + 2Me_3) - \frac{r^2_1 - M^2}{-k^2_{1\perp} - M^2} \\ &\quad \times \Bigg[V(-r_{3\perp}, k_{2\perp}) + \left(2 - \frac{1}{2^{N_3 - 1}}\right) Me_3 - \frac{r^2_3 - \left(2 - \frac{1}{2^{N_3 - 1}}\right) M^2}{-k^2_{2\perp} - M^2} \\ &\quad \times (V(k_{2\perp}, k_{2\perp}) + 2Me_3) \Bigg]^T \Bigg\} \end{aligned} \tag{A.14}$$

For the scattering process in the (ab) channel (exchange of N_4 vector particles) we have, at the central vertex, the matrix $R(k_{2\perp}, k_{3\perp})(H_{vv})^{N_4}$. In order to return to the (abc) c.m.s., we use the matrix $L_{ab}(k_3)$. The calculations are straightforward, and the results are illustrated in fig. 22.

From these two steps we already recognize the general pattern: each time when we switch from the (bc) c.m.s. to the (ab) c.m.s. (or vice versa), we double the number of terms. There is one group of contributions (e.g., the first and third terms of fig. 22) in which the new exchanges in the (ab) channel couple directly to the previous result; in the other group of contributions (e.g., the second and fourth terms of fig. 22) there is a propagator line between the new exchanges and the previous results, accompanied by the factor $(R^2 - \alpha M^2)/(k_2^2 + M^2)$ in our formula (R is the total momentum carried by the previously exchanged particles, e.g., $r_2 + r_3$, r_1, and r_3 in the second, third, and fourth term of fig. 22, respectively: k_2 is the momentum along this propagator line; for the factor α in front of M^2 we do not want to give an explicit rule, for reasons which we shall explain below). Higgs scalars only occur within a circle of fig. 22, i.e., the link lines between circles always belong to vector particles. When adding their contributions to those of the vector particles, one only changes the factor α for that vertex in which the Higgs scalar is produced.

Finally, we come to the right end of fig. 20. From the previous step we have terms like (cf. fig. 23; we are still in the (bc) c.m.s.):

$$(-i)(-1)^{N_3+\cdots+N_{n-2}}\left\{V(r_{i\perp}, k_{n-1\perp}) - c_1 M e_3 - \frac{r_i^2 - c_2 M^2}{-k_{n-2\perp}^2 - M^2} \times (V(k_{n-2\perp}, k_{n-2\perp}) - c_3 M e_3)\right\}^{T}. \qquad \text{(A.15)}$$

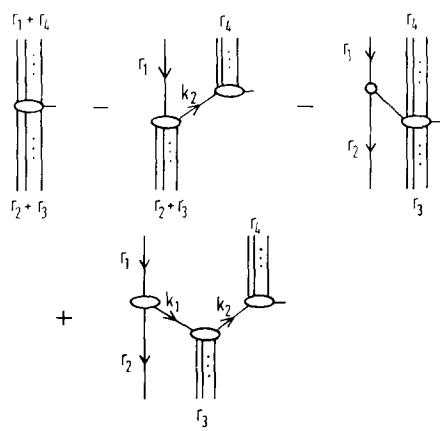

Fig. 22. Momentum structure of the production vertex (A.14).

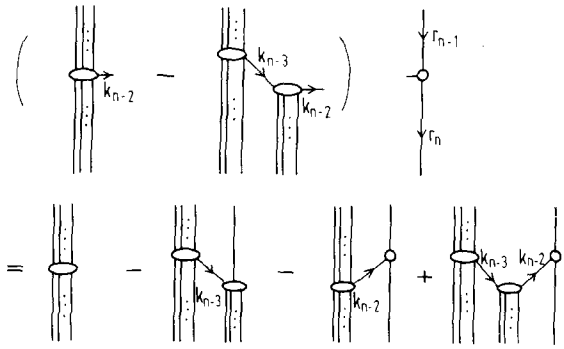

Fig. 23. Momentum structure of (A.17).

For the r.h.s. production vertex of fig. 20 we also go into the (bc) c.m.s.:

$$(-i)\Big\{ V(r_{n-1\perp}, -k_{n-1\perp}) - Me_3 - \frac{r_{n-1}^2 - M^2}{-k_{n-1\perp}^2 - M^2}\big(V(-k_{n-1\perp}, k_{n-1\perp}) - 2Me_3\big)\Big\}^{\mathrm{T}}. \tag{A.16}$$

Putting together eqs. (A.15) and (A.16) we arrive at (fig. 23)

$$2(-1)^N\Big\{(r_i + r_{n-1})_\perp^2 + \alpha_1 M^2 - \frac{(r_i^2 - c_2M^2)\big((r_{n-1\perp} + k_{n-2\perp})^2 + \alpha_2 M^2\big)}{-k_{n-2\perp}^2 - M^2} - \frac{(r_{n-1}^2 - c_2M^2)\big((r_i - k_{n-1})_\perp^2 + \alpha_3 M^2\big)}{-k_{n-1\perp}^2 - M^2} - \frac{(r_i^2 - c_2M^2)(r_{n-1}^2 - M^2)\big((k_{n-2} - k_{n-1})_\perp^2 + \alpha_1 M^2\big)}{(-k_{n-2\perp}^2 - M^2)(-k_{n-1\perp}^2 - M^2)}\Big\} \tag{A.17}$$

($N = N_3 + \cdots N_{n-2} + 1$ is the total number of intermediate states in fig. 20). Our previous remark that switching from the (ab) c.m.s. to the (bc) c.m.s. doubles the number of terms remains true; the same holds for the final connections with the right-hand vertex.

This completes our description of the algebra one has to do in order to obtain the momentum structure of a production vertex. The reason why we have not been very specific about the contribution of Higgs production along the central line in fig. 20 and constants in front of terms proportional to M^2 in the numerators is the

following. Since we are mostly interested in the vacuum exchange channel, and since the leading j-plane singularity in this channel comes from the large momentum region (this is explained in refs. [10, 5, 6]), we can restrict ourselves to large values of the momenta or, equivalently, to the limit $M^2 \to 0$. In this limit, terms proportional to M^2 become unimportant, and we can forget about the Higgs scalars. Moreover, the terms coming from the vector particle production can be combined to a very simple expression. The final result for the central part of fig. 22 is:

$$\left(r_1 - k_1 \frac{r_1^2}{k_1^2}\right)_i T_{ij}(k_1) T_{jl}(k_2) \ldots T_{rs}(k_{n-2}) \left(r_{n-1} + k_{n-2} \frac{r_{n-1}^2}{k_{n-1}^2}\right)_s , \qquad \text{(A.18)}$$

where

$$T_{ij}(k) = \delta_{ij} - 2 \frac{k_i k_j}{k^2} . \qquad \text{(A.19)}$$

This expression will be used in the following parts of our program.

References

[1] J. Bartels, Nucl. Phys. B151 (1979) 293
[2] V.S. Fadin, E.A. Kuraev and L.N. Lipatov, Phys. Lett. 60B (1975) 50
[3] C.Y. Lo and H. Cheng, Phys. Rev. D15 (1977) 2959
[4] M.T. Grisaru, H.J. Schnitzer and H.-S. Tsao, Phys. Rev. D8 (1973) 4498
[5] J. Bartels, Proceedings 10th GIFT Seminar on Theoretical physics, Jaca, Spain, June, 1979; 9th Int. Summer Inst. on Theoretical physics, Kaiserslautern, W. Germany, August, 1979; Acta Phys. Pol. B11 (1980) 281
[6] J. Bartels, DESY 80/54
[7] V.N. Gribov, JETP (Sov. Phys.) 26 (1968) 414;
J. Bartels, Phys. Rev. D11 (1975) 2977
[8] L.N. Lipatov, Yad. Fiz. 23 (1976) 642 (Sov. J. Nucl. Phys. 23 (1976) 338)
[9] C.Y. Lo and H. Cheng, Phys. Rev. D13 (1976) 1131
[10] E.A. Kuraev, L.N. Lipatov and V.S. Fadin, JETP (Sov. Phys.) 72 (1977) 377
[11] Ya.Ya. Balitsky, L.N. Lipatov and V.S. Fadin, Materials of the 14th Winter School of the Leningrad Inst. of Nuclear Research, 1979, p. 109
[12] H. Cheng, J. Dickinson, C.Y. Lo, K. Olausen and P.S. Yeung, Phys. Lett. 76B (1978) 129;
H. Cheng, J. Dickinson, C.Y. Lo and K. Olausen, preprint (1977); Stony Brook ITP-SB-79-7
[13] P. Carruthers, Introduction to unitary symmetry (Interscience, 1966)
[14] A.R. White, Nucl. Phys. B159 (1979) 77